Tight Upper Bounds on the BLER of Spinal codes over the AWGN Channel

Aimin Li [ID], Shaohua Wu [ID], *Member, IEEE*, Xiaomeng Chen [ID], and Sumei Sun [ID], *Fellow, IEEE*

Abstract—This paper establishes an upper bound on the block error rate (BLER) of Spinal codes, the first rateless codes proven to achieve Shannon capacity in additive white Gaussian noise (AWGN) and binary symmetric channels (BSC). Unlike the conventional reliance on the *1965 Gallager random coding bound* [1, *Theorem 5.6.2*] for deriving upper bounds, as illustrated in 2016 [2] by Yu *et. al*, this study deviates by noting that Gallager's bound may not adequately represent the distinct properties of specific random codes like Spinal codes and may result in loose bounding performance. We thus introduce novel techniques to refine existing results and enhance the bounding tightness. Our main results are two explicit upper bounds on the BLER of Spinal codes over the AWGN channel, accompanied by theoretical proofs that validate their tightness. Potential applications of the bounds and insights for the coding design are explored in this work.

Index Terms—Spinal codes, decoding error probability, ML decoding, upper bounds, rateless codes.

I. INTRODUCTION

A. Background

SPINAL code is a *capacity-achieving* channel coding technique that has been proved to asymptotically achieve the Shannon capacity over both the additive white Gaussian noise (AWGN) channel and the binary symmetric channel (BSC) [3]. The exceptional performance of Spinal codes stems from the combination of hash functions and Random Number Generators (RNGs), which provide Spinal code with superior code rate performance across wide range of channel conditions. In [4] and [5], it has been shown that rateless Spinal

A. Li is with the Guangdong Provincial Key Laboratory of Aerospace Communication and Networking Technology, Harbin Institute of Technology (Shenzhen), Shenzhen 518055, China, and also with the Institute for Infocomm Research, Agency for Science, Technology and Research, 138632, Singapore. E-mail: liaimin@stu.hit.edu.cn.

S. Wu is with the Guangdong Provincial Key Laboratory of Aerospace Communication and Networking Technology, Harbin Institute of Technology (Shenzhen), Shenzhen 518055, China, and also with the Pengcheng Laboratory, Shenzhen 518055, China (e-mail: hitwush@hit.edu.cn).

X. Chen is with the Department of Electronic Engineering, Harbin Institute of Technology (Shenzhen), Shenzhen, China 518055. E-mail: 23s052026@hit.edu.cn.

S. Sun is with the Institute for Infocomm Research, Agency for Science, Technology and Research (A*STAR), Singapore 138632. Email: sunsm@i2r.a-star.edu.sg.

codes exhibit higher rate performance compared to fixed-rate Low-Density Parity-Check (LDPC) codes [6], rateless Raptor codes [7], and layered rateless Strider codes [8], across a wide range of channel conditions and message sizes.

With outstanding rate performance for short message lengths and a natural adaptability to time-varying channel conditions, Spinal codes have shown significant potential for deployment in 6G non-terrestrial networks (NTN) [9], such as deep space exploration [10], [11], UAV networks [12]–[15], and satellite laser communications [16]. Numerous coding-decoding algorithms are designed to improve the performance of Spinal codes. Such explorations include the application of puncturing on Spinal codes [17], [18], coding structure improvements [2], [19]–[23], concatenation with outer codes [24]–[27], Compressive Spinal codes [28], low-complexity decoding algorithms [29]–[31], and block assignments for timeliness-oriented Spinal codes [32], [33]. These advancements have notably improved the performance of Spinal codes. However, a comprehensive theoretical analysis of their mechanisms remains a challenge and an area that is under-researched. Within the broader domain of channel coding, the analysis of error probability bounds remains a critical focus, encompassing studies on Raptor codes [34], Polar codes [35], [36], and LT codes [37], [38], as well as on the error probability of Maximum Likelihood (ML)-decoded linear codes [39]. The theoretical exploration of emerging techniques like Spinal codes, however, is still in its early stages.

B. Related Works and Contributions

The first work analyzing the performance of Spinal codes was conducted by their creator, as detailed in [3]. This seminal work presented an asymptotic rate performance analysis of Spinal codes, theoretically demonstrating their capacity-achieving properties over both the AWGN channel and the BSC. Subsequently, in [2], Yu *et al.* extended this asymptotic analysis to finite block-length (FBL) analysis and analyzed the upper bound on the error probability of Spinal codes. This analysis considered the tree structure of Spinal codes and applied existing bounding techniques for pairwise independent random codes, specifically the *Random Coding Union* (RCU) bound and the 1965 *Gallager random coding bound* to derive the upper bound on Spinal codes. However, the reliance on these bounds may not fully reflect the unique properties of Spinal codes, potentially leading to less precise evaluations.

In our previous works [22], [23], we established an upper bound on the BLER of Spinal codes over Rayleigh fading

channels. This analysis utilized the *union bound of probability*, the *Chernoff bound*, and the *geometric probability* for bounding the BLER of Spinal codes. However, the application of the *Chernoff bound* resulted in derived bounds that were not in a strictly closed form. Instead, these bounds exhibited probabilistic convergence, indicating that they are valid with a confidence probability less than one.

Motivated by the above, this work aims to address an essential yet unexplored question: *Is it possible to explore Spinal codes' intrinsic properties more deeply to obtain precise, closed-form error probability bounds over the AWGN channel, without resorting to the 1965 Gallager random coding bound?* Central to this challenging problem, the main contributions of this paper are two rigorously closed-form upper bounds on the error probability of Spinal codes over the AWGN channel. We conduct Monte Carlo simulations to verify that our proposed bounds are tighter. Furthermore, we provide a theoretical proof that our explicit bounds 1 exhibit improved tightness compared to the explicit bound in [2, *Theorem 4*]. Potential applications of the bound are explored in the paper.

II. PRELIMINARIES OF SPINAL CODES
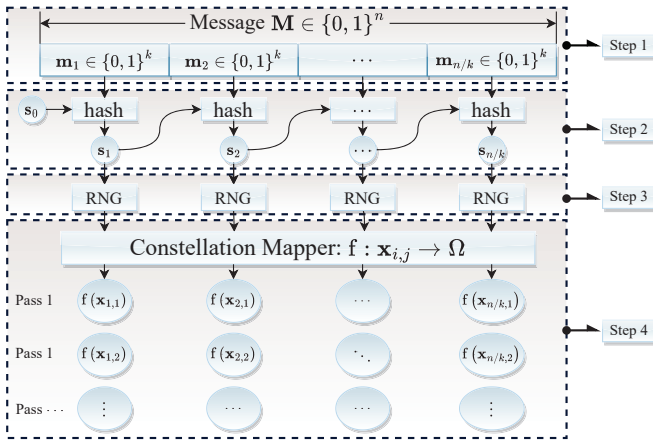
A. Coding Process of Spinal Codes

Fig. 1. The encoding process of Spinal codes.

Fig. 1 illustrates the encoding process of Spinal codes:

1) An n-bit message $\mathbf{M}$ is divided into k-bit segments, denoted by $\mathbf{m}_i$, where $i = 1, 2, \ldots, n/k$.
2) An iterative process is invoked to generate v-bit spine values $\mathbf{s}_i \in \{0,1\}^v$:

$$\mathbf{s}_i = h(\mathbf{s}_{i-1}, \mathbf{m}_i), i = 1, \ldots, n/k, \mathbf{s}_0 = \mathbf{0}^v.\text{[1]} \quad (1)$$

3) The v-bit spine value $\mathbf{s}_i$ serves as a seed of an RNG to generate a pseudo-random uniform-distributed sequence $\{\mathbf{x}_{i,j}\}$:

$$\text{RNG} : \mathbf{s}_i \to \{\mathbf{x}_{i,j}\}, \mathbf{x}_{i,j} \in \{0,1\}^c, j = 1, 2, 3, \cdots, \quad (2)$$

---

[1] The initial spine value $\mathbf{s}_0$ is known to both the encoder and the decoder. Without loss of generality, we set $\mathbf{s}_0 = \mathbf{0}^v$ in this paper.

4) The constellation mapper maps each c-bit symbol to a channel input set Ω:

$$\text{f} : \mathbf{x}_{i,j} \to \Omega, \quad (3)$$

where f is a constellation mapping function and Ω denotes the channel input set.

In general, Spinal codes exhibit the following important features that contribute to their performance superiority:

Lemma 1. *(Pairwise independent property) As Perry* et al. *indicat in [5], the hash function employed by Spinal codes should have pairwise independent property:*

$$\begin{aligned} &\Pr\left\{h\left(\mathbf{s}, \mathbf{m}\right) = \mathbf{x}, h\left(\mathbf{s}', \mathbf{m}'\right) = \mathbf{x}'\right\} \\ &= \Pr\left\{h\left(\mathbf{s}, \mathbf{m}\right) = \mathbf{x}\right\} \cdot \Pr\left\{h\left(\mathbf{s}', \mathbf{m}'\right) = \mathbf{x}'\right\} \\ &= 2^{-2v}, \end{aligned} \quad (4)$$

where $(\mathbf{s}, \mathbf{m})$ *and* $(\mathbf{s}', \mathbf{m}')$ *are two different inputs of the hash function. This characteristics is crucial for the BLER analysis.*

Definition 1. *A hash collision occurs when two different inputs of the hash function produce the same output,* i.e., $h(\mathbf{s}, \mathbf{m}) = h(\mathbf{s}', \mathbf{m}')$ *while* $(\mathbf{s}, \mathbf{m}) \neq (\mathbf{s}', \mathbf{m}')$.

Corollary 1. *The probability of hash collisions decreases exponentially with the hash parameter* v, *i.e.,* $\Pr\{h(\mathbf{s}, \mathbf{m}) = h(\mathbf{s}', \mathbf{m}')\} = 2^{-v}$, *where* $(\mathbf{s}, \mathbf{m})$ *and* $(\mathbf{s}', \mathbf{m}')$ *are two different inputs.*

Proof. See Appendix A. ■

B. ML Decoding Process of Spinal Codes

The ML decoding rule for Spinal codes is:

$$\hat{\mathbf{M}} \in \underset{\mathbf{M}' \in \{0,1\}^n}{\arg\min} \mathscr{D}(\mathbf{M}'), \quad (5)$$

where $\mathscr{D}(\mathbf{M}')$ is the decoding cost defined as:

$$\mathscr{D}(\mathbf{M}') \triangleq \sum_{i=1}^{n/k} \sum_{j=1}^{L} (y_{i,j} - \text{f}(\mathbf{x}_{i,j}(\mathbf{M}')))^2, \quad (6)$$

with $y_{i,j} = \text{f}(\mathbf{x}_{i,j}(\mathbf{M}')) + n_{i,j}$ representing the received symbols over the AWGN channel, $\hat{\mathbf{M}}$ representing the decoding result, $\mathbf{M}'$ representing the candidate sequence, and L denoting the number of transmitted passes for Spinal codes. In ML decoding, the ML decoder adopts i) the shared knowledge of the same hash function, ii) the same initial spine value $\mathbf{s}_0$ and iii) the same RNG to replay the coding process over the candidate sequences set $\{0,1\}^n$.

C. Upper Bounds Based on 1965 Gallager Random Coding Bound

This subsection reviews the BLER analysis for Spinal codes presented in [2]. In this work, the analysis employs the 1965 *Gallager Random Coding Bound*, with a specific substitution $\rho = 1$ as one of the core steps to obtain the bound. The bound in [2] is given in the following Theorem.

Theorem 1. *(Restatement of [2, Theorem 4]) Consider Spinal codes with message length* n *and segmentation parameter* k *transmitted over an AWGN channel with noise variance* σ^2.

This article has been accepted for publication in IEEE Transactions on Communications. This is the author's version which has not been fully edited and content may change prior to final publication. Citation information: DOI 10.1109/TCOMM.2024.3435391

3

Let L be the number of transmitted passes. The average BLER under ML decoding can be upper bounded by

$$P_e \leq 1 - \prod_{a=1}^{n/k} (1 - \epsilon_a), \tag{7}$$

with

$$\epsilon_a = \exp\left\{ -L_a \cdot \left[E_o(\mathcal{Q}) - \frac{\ln U_a}{L_a} \right] \right\}, \tag{8}$$

where $L_a = L(n/k - a + 1)$, $U_a = 2^{k(n/k-a+1)}$, $\mathcal{Q}$ denotes the probability distribution of the channel input and

$$E_0(\mathcal{Q}) = -\ln\left\{ \frac{1}{\sqrt{2\pi\sigma^2}} \times \int_{\mathbb{R}} \left(\sum_{x\in\Omega} \mathcal{Q}(x) \cdot \exp\left(-\frac{(y-x)^2}{4\sigma^2}\right) \right)^2 dy \right\}, \tag{9}$$

where Ω is the channel input set.

In the proof of Theorem 1, the 1965 *Gallager random coding bound* [1, *Theorem 5.6.2*] is employed, which is $P_e \leq \exp\{-L \cdot E_r(R)\}$, with

$$E_r(R) = \max_{0\leq\rho\leq 1} (E_o(\mathcal{Q},\rho) - \rho R) \tag{10}$$

and

$$E_o(\mathcal{Q},\rho) = -\ln\left\{ \int_{\mathbb{R}} \left[\sum_{x\in\Omega} \mathcal{Q}(x) P(y\mid x)^{1/(1+\rho)} \right]^{1+\rho} dy \right\}. \tag{11}$$

However, it is hard to explicitly calculating $E_0(\mathcal{Q},\rho)$, making the determination of $E_r(R)$ challenging. To address this, the authors in [2] resorted to a relaxed variant to establish (8):

$$\begin{aligned} P_e &\leq \exp\left\{ -L \cdot \left[\max_{0\leq\rho\leq 1} (E_0(\mathcal{Q},\rho) - \rho R) \right] \right\} \\ &= \min_{0\leq\rho\leq 1} \{\exp[-L \cdot (E_0(\mathcal{Q},\rho) - \rho R)]\} \\ &\leq \exp\{-L \cdot (E_0(\mathcal{Q}) - R)\}, \end{aligned} \tag{12}$$

where $E_0(\mathcal{Q},1) = E_0(\mathcal{Q})$ and $R = \frac{\ln U_a}{L_a}$. In (12), the second inequality derives from that for any functions $f(\cdot)$, the inequality $\min_{0\leq\rho\leq 1} f(\rho) \leq f(1)$ always holds true. The bound (12) leads to the bound (8) in Theorem 1.

When applying the 1965 *Gallager random coding bound*, the authors in [2] set ρ as 1 to upper bound $E(\mathcal{Q},\rho)$ and $E_r(R)$. However, the right-hand side (RHS) of (9) involves integrating the square of a summation, which still presents calculation complexity. Consequently, we here refine the inner integration within (9) and express it as more compact form:

(see Appendix B for the detailed proof)

$$E_0(\mathcal{Q}) = -\ln\left\{ 2^{-2c} \times \sum_{j\in\Omega}\sum_{i\in\Omega} \exp\left(-\frac{(i-j)^2}{8\sigma^2} \right) \right\}. \tag{13}$$

With (13), $E_0(\mathcal{Q})$ can be determined by calculating the logarithm of the summation $\exp\{-\frac{(i-j)^2}{8\sigma^2}\}$ over $i,j \in \Omega$.

III. BOUND BASED ON GEOMETRIC PROBABILITY

The purpose of this work is to tighten the bound illustrated in [2]. Since the bound in [2] applies an relaxed variant of the 1965 *Gallager random coding bound* [1, *Theorem 5.6.2*] $P_e \leq 2^{-L\cdot(E(\mathcal{Q},\rho)-\rho R)}$ by substituting $\rho = 1$, one straightforward way to tighten the bound is to eliminate the relaxation $\min_{0\leq\rho\leq 1} f(\rho) \leq f(1)$ and explicitly derive $E_r(R)$ in a closed form. However, this poses significant challenges. As noted in [1, *Example 1, Page 146*], "*Even for a simple channel like the binary symmetric channel, there is no simple way to express $E_r(R)$ except in parametric form.*" This impedes the development of tight explicit bounds for Spinal codes.

In this paper, we bypass the necessity for the 1965 *Gallager random coding bound* and reestablish a tighter upper bound. We establish the first bound on BLER of Spinal codes through the *geometric probability* [40]. Through this approach, we transform a conditional probability into the ratio of volumes of two hyper geometric objects (see Fig. 2 and Lemma 3). The explicit bound based on this technique is outlined in Section III-A with a proof provided in Section III-B.

A. Explicit Upper Bound on BLER

Theorem 2. *(Bound based on geometric probability) Consider Spinal codes with message length n, segmentation parameter k, modulation parameter c, and sufficiently large hash parameter v transmitted over an AWGN channel with SNR γ. The average BLER under ML decoding for Spinal codes can be upper bounded by*

$$P_e \leq 1 - \prod_{a=1}^{n/k} (1 - \epsilon_a), \tag{14}$$

with

$$\epsilon_a = \min\left\{ 1, \left(2^k - 1\right) 2^{n-ak} \cdot \mathscr{F}(L_a, \gamma) \right\}, \tag{15}$$

and

$$\mathscr{F}(L_a, \gamma) = \frac{\pi^{L_a/2} L_a \mathscr{H}(L_a, \gamma)}{\Gamma^2\left(1 + \frac{L_a}{2}\right)\left(\sqrt{24\gamma}\right)^{L_a}} + \frac{L_a \mathscr{G}(L_a, \gamma)}{\Gamma\left(1 + \frac{L_a}{2}\right)\left(\sqrt{2}\right)^{L_a}}, \tag{16}$$

where $L_a \triangleq L \cdot (n/k - a + 1)$ represents the cumulative transmitted symbols from the ath segment to the $(n/k)^{\text{th}}$

$$\mathscr{G}(L_a, \gamma) = \begin{cases} \exp\left[\frac{-\beta^2(L_a,\gamma)}{2}\right] \sum_{i=1}^{L_a/2} \beta(L_a,\gamma)^{L_a-2i} \mathcal{K}_{i-1}, & \text{if } L_a \text{ is even} \\ \sigma^{L_a}\left(\sqrt{2\pi}Q\left(\beta(L_a,\gamma)\right)\mathcal{K}_{(L_a-3)/2} + \exp\left[\frac{-\beta^2(L_a,\gamma)}{2}\right] \sum_{i=1}^{(L_a-1)/2} \beta(L_a,\gamma)^{L_a-2i} \mathcal{K}_{i-1}\right), & \text{if } L_a \text{ is odd} \end{cases}, \tag{18}$$

segment, $\mathscr{H}(L_a, \gamma)$ is given as

$$\mathscr{H}(L_a, \gamma) = -e^{\frac{-\beta(L_a, \gamma)^2}{2}} \sum_{i=1}^{L_a} \beta(L_a, \gamma)^{2(L_a - i)} \mathcal{I}_{i-1} + \mathcal{I}_{L_a - 1},$$
(17)

$\mathscr{G}(L_a, \gamma)$ is given in (18) at the bottom of this page, with

$$\beta(L_a, \gamma) = \sqrt{\frac{12\gamma}{\pi}} \Gamma(1 + L_a/2)^{1/L_a}.$$
(19)

In the above expressions, $\Gamma(\cdot)$ denotes the Gamma function, $\mathcal{I}_i$ is defined as $\mathcal{I}_i \triangleq \prod_{j=1}^{i} 2(L_a - j)$, and $\mathcal{K}_i$ is given by $\mathcal{K}_i \triangleq \prod_{j=1}^{i}(L_a - 2j)$.

B. Proof of Theorem 2

Theorem 2 establishes an explicit bound on ML-decoded Spinal codes. To derive this bound, we first decompose the BLER P_e into products of conditional error probabilities, as detailed in Section III-B1. We then explore the geometric interpretations of these conditional error probabilities using a *geometric probability* in Section III-B2, where we demonstrate that the conditional error probability can be represented by the ratio of volumes of two specific geometric objects. Third, we recognize that to explicitly solving the volume of the hyper geometric object is non-trivial, and thus we upper bound the volume in Section III-B3. Finally, we employ Gaussian integration to explicitly calculate the bound in Section III-B4.

1) P_e Decomposition:

Denote $\mathcal{E}_a$ as the event that there exists a decoding error in the ath segment of Spinal codes and $\bar{\mathcal{E}}_a$ as the complement of $\mathcal{E}_a$. The BLER of Spinal codes can be decomposed through the *multiplication rule of probability*:

$$P_e = \Pr\left\{\bigcup_{a=1}^{n/k} \mathcal{E}_a\right\} = 1 - \Pr\left\{\bigcap_{a=1}^{n/k} \bar{\mathcal{E}}_a\right\}$$
$$= 1 - \prod_{a=1}^{n/k} \left(1 - \Pr\left\{\mathcal{E}_a \left| \bigcap_{j=1}^{a-1} \bar{\mathcal{E}}_j\right.\right\}\right).$$
(20)

For concise notations, denote ϵ_a as the conditional probability

$$\epsilon_a = \Pr\left\{\mathcal{E}_a \left| \bigcap_{j=1}^{a-1} \bar{\mathcal{E}}_j\right.\right\}.$$
(21)

Our primary objective is to formulate an explicit upper bound on ϵ_a, thus establishing the upper bound on P_e.

2) Upper Bound ϵ_a: A Geometric Probability Approach

Suppose message $\mathbf{M} = (\mathbf{m}_1, \mathbf{m}_2, \ldots, \mathbf{m}_{n/k}) \in \{0, 1\}^n$ is encoded to Spinal codewords $\mathrm{f}(\mathbf{x}_{i,j}(\mathbf{M}))$ for transmission over an AWGN channel. Let $y_{i,j}$ denote the corresponding received symbol at the receiver, and denote $n_{i,j}$ as the AWGN with variance σ^2. The received symbol is $y_{i,j} = \mathrm{f}(\mathbf{x}_{i,j}(\mathbf{M})) + n_{i,j}$. Define $\mathcal{W}_a \triangleq \{(\mathbf{m}'_1, \ldots, \mathbf{m}'_{n/k}) : \mathbf{m}'_1 = \mathbf{m}_1, \ldots, \mathbf{m}'_{a-1} = \mathbf{m}_{a-1}, \mathbf{m}'_a \neq \mathbf{m}_a\}$ as the set of messages where the first $a-1$ segments are identical to those of $\mathbf{M}$, but the a-th segment differs.

From the ML decoding rule given in (5), we know that a conditional error occurs when a candidate sequence $\mathbf{M}' \in \mathcal{W}_a$ exists such that its decoding cost $\mathscr{D}(\mathbf{M}')$ is lower than the correct sequence's decoding cost $\mathscr{D}(\mathbf{M})$, *i.e.*, $\exists \mathbf{M} \in \mathcal{W}_a, \mathscr{D}(\mathbf{M}') < \mathscr{D}(\mathbf{M})$. Thus, the conditional probability ϵ_a is expressed as

$$\epsilon_a = \Pr\left\{\mathcal{E}_a \left| \bigcap_{j=1}^{a-1} \bar{\mathcal{E}}_j\right.\right\} = \Pr\{\exists \mathbf{M}' \in \mathcal{W}_a : \mathscr{D}(\mathbf{M}') \leq \mathscr{D}(\mathbf{M})\}.$$
(22)

Applying the *union bound of probability* yields:

$$\Pr\{\exists \mathbf{M}' \in \mathcal{W}_a : \mathscr{D}(\mathbf{M}') \leq \mathscr{D}(\mathbf{M})\}$$
$$\leq \min\{1, \sum_{\mathbf{M}' \in \mathcal{W}_a} \Pr\{\mathscr{D}(\mathbf{M}') \leq \mathscr{D}(\mathbf{M})\}\},$$
(23)

where $\sum_{\mathbf{M}' \in \mathcal{W}_a} \Pr\{\mathscr{D}(\mathbf{M}') \leq \mathscr{D}(\mathbf{M})\}$ can be expanded by substituting the definition of $\mathscr{D}(\cdot)$ in (6):

$$\sum_{\mathbf{M}' \in \mathcal{W}_a} \Pr\left\{\sum_{i=1}^{n/k}\sum_{j=1}^{L}(y_{i,j} - \mathrm{f}(\mathbf{x}_{i,j}(\mathbf{M}')))^2 \leq \sum_{i=1}^{n/k}\sum_{j=1}^{L} n_{i,j}^2\right\}.$$
(24)

Next, we simplify (24) through the following Lemma.

Lemma 2. *The following assertions are true:*
(i). If $1 \leq i < a$ and $\mathbf{M}' \in \mathcal{W}_a$, we have $y_{i,j} - \mathrm{f}(\mathbf{x}_{i,j}(\mathbf{M}'))^2 = n_{i,j}^2$.
(ii). If $a \leq i \leq n/k$ and $\mathbf{M}' \in \mathcal{W}_a$, then $\mathrm{f}(\mathbf{x}_{i,j}(\mathbf{M}'))$ is independent with $y_{i,j}$.

Proof. See Appendix C. ∎

In Lemma 2, the assertion (i) simplifies (24) as:

$$\sum_{\mathbf{M}' \in \mathcal{W}_a} \Pr\left\{\sum_{i=a}^{n/k}\sum_{j=1}^{L}(y_{i,j} - \mathrm{f}(\mathbf{x}_{i,j}(\mathbf{M}')))^2 \leq \sum_{i=a}^{n/k}\sum_{j=1}^{L} n_{i,j}^2\right\}.$$
(25)

We next show that the assertion (ii) of Lemma 2 enables us to employ *geometric probability* for analyzing the RHS of (25). By introducing $\mathbf{y}^{L_a}$ as the vector comprising $y_{i,j}$ with $a \leq i \leq n/k, 1 \leq j \leq L$, $\mathbf{X}^{L_a}(\mathbf{M}')$ as the vector comprising $\mathrm{f}(\mathbf{x}_{i,j}(\mathbf{M}'))$, and $\mathbf{N}^{L_a}$ as the vector comprising $n_{i,j}$ with $a \leq i \leq n/k, 1 \leq j \leq L$, where $L_a = L(n/k - a + 1)$, (25) can be then expressed in a vector form:

$$\sum_{M' \in \mathcal{W}_a} \overbrace{\int_{\mathbb{R}} \cdots \int_{\mathbb{R}}}^{L_a} \Pr\left\{\left\|\mathbf{y}^{L_a} - \mathbf{X}^{L_a}(\mathbf{M}')\right\|^2 \leq \right.$$
$$\left.\left\|\mathbf{n}^{L_a}\right\|^2 \left|\mathbf{N}^{L_a} = \mathbf{n}^{L_a}\right.\right\} \prod_{i=a}^{n/k} \Pr(\mathbf{N}^{L_a} = \mathbf{n}^{L_a}) d\mathbf{n}^{L_a}.$$
(26)

The results from *geometric probability* is summarized in the following Lemma.

Lemma 3. *The conditional probability in (26), given as $\Pr\{\|\mathbf{y}^{L_a} - \mathbf{X}^{L_a}(\mathbf{M}')\|^2 \leq \|\mathbf{n}^{L_a}\|^2 | \mathbf{N}^{L_a} = \mathbf{n}^{L_a}\}$, can be ap-*
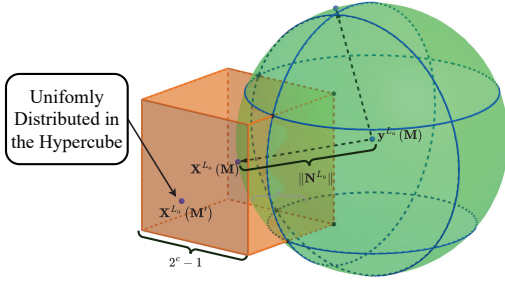
Fig. 2. A three-dimension (3D, $L_a = 3$) example of the relationship among $\mathbf{X}^{L_a}(\mathbf{M})$, $\mathbf{X}^{L_a}(\mathbf{M}')$, $\mathbf{N}^{L_a}$ and $\mathbf{y}^{L_a}(\mathbf{M})$.

proximated through the geometric probability, given as

$$\frac{\mathrm{Vol}\left[\mathbb{S}^{L_a}\left(\mathbf{y}^{L_a}(\mathbf{M}), \|\mathbf{n}^{L_a}\|\right) \bigcap \mathbb{C}^{L_a}(2^c-1)\right]}{\mathrm{Vol}\left(\mathbb{C}^{L_a}(2^c-1)\right)}, \quad (27)$$

where $\mathbb{S}^n(\mathbf{y}^n, r) \triangleq \left\{\mathbf{x}^n = (x_1, \cdots, x_n) \in \mathbb{R}^n | \|\mathbf{x}^n - \mathbf{y}^n\|^2 \leq r^2\right\}$, $\mathbb{C}^n(l) \triangleq \left\{\mathbf{x}^n = (x_1, \cdots, x_n) \in \mathbb{R}^n | 0 \leq x_i \leq l, \text{for } i \in [n]\right\}$ [^2], and $\mathrm{Vol}(x)$ represents the volume of the object x.

Proof. From the assertion (ii) of Lemma 2, it turns out that $\mathbf{X}^{L_a}(\mathbf{M}')$ is independent of $\mathbf{y}^{L_a}$. In this way, given a known $\mathbf{y}^{L_a}$, each element in $\mathbf{X}^{L_a}(\mathbf{M}')$ follows the uniform distribution with $\mathrm{f}(\mathbf{x}_{i,j}(\mathbf{M}')) \sim \mathtt{Uniform}[0, 2^c-1]$. This indicates that the vector $\mathbf{X}^{L_a}(\mathbf{M}')$ is uniformly distributed in an L_a-dimension hypercube, as shown in Fig. 2. As such, the probability $\Pr\left\{\|\mathbf{y}^{L_a} - \mathbf{X}^{L_a}(\mathbf{M}')\|^2 \leq \|\mathbf{n}^{L_a}\|^2 \mid \mathbf{N}^{L_a} = \mathbf{n}^{L_a}\right\}$ can be approximated as the volume of the intersection region between a L_a-dimension hypercube $\mathbb{C}^{L_a}(2^c-1)$ and a L_a-dimension hypersphere $\mathbb{S}^{L_a}\left(\mathbf{y}^{\mathbf{L_a}}(\mathbf{M}), \|\mathbf{n}^{\mathbf{L_a}}\|\right)$, divided by the volume of the hypercube $\mathbb{C}^{L_a}(2^c-1)$. ∎

3) Upper Bound the Ratio (27)

Lemma 3 reinterprets the probability into volumes of two hyper objects: (i) the intersection of the hypersphere and the hypercube $\mathbb{S}^{L_a}\left(\mathbf{y}^{L_a}(\mathbf{M}), \|\mathbf{n}^{L_a}\|\right) \bigcap \mathbb{C}^{L_a}(2^c-1)$; (ii) the hypercube $\mathbb{C}^{L_a}(2^c-1)$. Solving the volume of the intersection is non-trivial, and we thus establish an upper bound for it instead in the following.

As the volume of the intersection part does not surpass their individual volumes, *i.e.*, $\mathrm{Vol}(A) \cap \mathrm{Vol}(A) \leq \min\{\mathrm{Vol}(A), \mathrm{Vol}(B)\}$, we establish the bound:

$$\frac{\mathrm{Vol}\left[\mathbb{S}^{L_a}\left(\mathbf{y}^{L_a}(\mathbf{M}), \|\mathbf{n}^{L_a}\|\right) \bigcap \mathbb{C}^{L_a}(2^c-1)\right]}{\mathrm{Vol}\left(\mathbb{C}^{L_a}(2^c-1)\right)}$$
$$\leq \frac{\min\left\{\mathrm{Vol}\left(\mathbb{S}^{L_a}\left(\mathbf{y}^{L_a}(\mathbf{M}), \|\mathbf{n}^{L_a}\|\right)\right), \mathrm{Vol}\left(\mathbb{C}^{L_a}(2^c-1)\right)\right\}}{\mathrm{Vol}\left(\mathbb{C}^{L_a}(2^c-1)\right)}$$
$$= \min\left\{\frac{\mathrm{Vol}\left(\mathbb{S}^{L_a}\left(\mathbf{y}^{L_a}(\mathbf{M}), \|\mathbf{n}^{L_a}\|\right)\right)}{\mathrm{Vol}\left(\mathbb{C}^{L_a}(2^c-1)\right)}, 1\right\}. \quad (28)$$

Then, substituting the following volume expressions

$$\mathrm{Vol}\left(\mathbb{S}^n(\mathbf{y}^n, r)\right) = \frac{\pi^{n/2}}{\Gamma\left(1+\frac{n}{2}\right)} r^n, \mathrm{Vol}\left(\mathbb{C}^n(l)\right) = l^n \quad (29)$$

[^2]: The notation $[n]$ is employed as a shorthand to represent the set $\{1, \cdots, n\}$.

into the RHS of (28) yields

$$\frac{\mathrm{Vol}\left(\mathbb{S}^{L_a}\left(\mathbf{y}^{L_a}(\mathbf{M}), \|\mathbf{n}^{L_a}\|\right)\right)}{\mathrm{Vol}\left(\mathbb{C}^{L_a}(2^c-1)\right)} = \frac{\left(\pi \sum_{i=a}^{n/k} \sum_{j=1}^{L} n_{i,j}^2\right)^{L_a/2}}{(2^c-1)^{L_a} \Gamma\left(1+\frac{L_a}{2}\right)}. \quad (30)$$

Applying (27)-(30) in (26) yields an explicit bound on ϵ_a:

$$\epsilon_a \leq \min\left\{1, \sum_{\mathbf{M}' \in \mathcal{W}_a} \underbrace{\int \cdots \int_{\mathbb{R}}}_{L_a} \min\left(1, \frac{\left(\pi \sum_{i=a}^{n/k} \sum_{j=1}^{L} n_{i,j}^2\right)^{L_a/2}}{(2^c-1)^{L_a} \Gamma\left(1+\frac{L_a}{2}\right)}\right) \times \right.$$
$$\left. \frac{1}{\left(\sqrt{2\pi\sigma^2}\right)^{L_a}} e^{\frac{-\sum_{i=a}^{n/k} \sum_{j=1}^{L} n_{i,j}^2}{2\sigma^2}} \prod_{i=a}^{n/k} \prod_{j=1}^{L} dn_{i,j}\right\}. \quad (31)$$

4) Closed-Form Solution to (31)

Our remaining focus is to solve the L_a-dimension integral on the RHS of (31). To address this challenge, we introduce *hyperspherical coordinates* and *Gaussian integrals* (refer to Appendix D) to simplify (31). The closed-form solution to (31) is outlined in Lemma 4.

Lemma 4. *The L_a-dimension integral in (31) can be rewritten as an analytical function of L_a and SNR γ, denoted by $\mathscr{F}(L_a, \gamma)$ given as:*

$$\mathscr{F}(L_a, \gamma) = \frac{\pi^{L_a/2} L_a \mathscr{H}(L_a, \gamma)}{\Gamma^2\left(1+\frac{L_a}{2}\right)\left(\sqrt{24\gamma}\right)^{L_a}} + \frac{L_a \mathscr{G}(L_a, \gamma)}{\Gamma\left(1+\frac{L_a}{2}\right)\left(\sqrt{2}\right)^{L_a}}, \quad (32)$$

where the closed-form expressions of functions $\mathscr{H}(L_a, \gamma)$ and $\mathscr{G}(L_a, \gamma)$ are given in (17)-(19).

Proof. See Appendix D. ∎

Substituting the explicit function $\mathscr{F}(L_a, \gamma)$ into (31) yields an closed-form upper bound on ϵ_a:

$$\epsilon_a \leq \min\left\{1, \sum_{\mathbf{M}' \in \mathcal{W}_a} \mathscr{F}(L_a, \gamma)\right\}$$
$$= \min\left\{1, |\mathcal{W}_a| \cdot \mathscr{F}(L_a, \gamma)\right\} \quad (33)$$
$$= \min\left\{1, \left(2^k-1\right) 2^{n-ak} \cdot \mathscr{F}(L_a, \gamma)\right\}.$$

As last, applying the bound on ϵ_a in (20) results in the upper bound on P_e outlined in Theorem 2.

IV. BOUND BASED ON CRAIG'S IDENTITY AND RULE OF RIEMANN RIGHT SUM

We observe that the the bound in Theorem 2 only achieves tight approximations under the high-SNR regime (See Section VI). This limitation motivates us to investigate the causes of this phenomenon. Subsequently, we provide an explanation for the limited accuracy of Theorem 2 in the low-SNR regime.
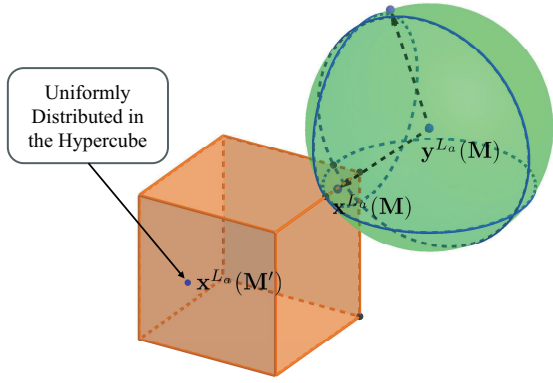
Fig. 3. An example where the bound (28) is overestimated.

Consider a scenario where the encoded symbol vector $\mathbf{X}^{L_a}(\mathbf{M})$ is at the boundary of the hypercube and the noise is very large, as shown in Fig. 3. In this case, the bound (28), which uses the volume of the hypersphere to upper bound the volume of the intersection, is significantly overestimated. This overestimation is prevalent under conditions of large noise, resulting in a reduced accuracy of the bound in low SNR regimes. To address the dynamics of $\mathbf{X}^{L_a}(\mathbf{M})$ and the resulting overestimation under low-SNR regime, we propose new analytical methods in this section.

In summary, this section establishes a new bound that incorporates the random dynamics of $\mathbf{X}^{L_a}(\mathbf{M})$. The key of the bound lies in the *Craig's Identity* $Q(x) = \frac{1}{\pi}\int_0^{\frac{\pi}{2}} \exp\left(\frac{-x^2}{2\sin^2\theta}\right) d\theta$ [41] and the *Rule of Right Riemann Sum*. The explicit bound is detailed in the subsequent theorem.

A. Explicit Upper Bound on BLER

Theorem 3. (***Bound Based on Craig's Identity and Rule of Riemann Right Sum***) *Consider Spinal codes with message length n, segmentation parameter k, modulation parameter c, and sufficiently large hash parameter v transmitted over an AWGN channel with variance σ^2. The average BLER under ML decoding can be upper bounded by*

$$P_e \leq 1 - \prod_{a=1}^{n/k}(1 - \epsilon_a), \quad (34)$$

with

$$\epsilon_a = \min\left\{1, \left(2^k - 1\right)2^{n-ak}\cdot\mathscr{F}_2\left(L_a, \sigma\right)\right\}, \quad (35)$$

$$\mathscr{F}_2\left(L_a, \sigma\right) = \sum_{r=1}^{N} b_i \mathcal{F}\left(\theta_r; \sigma, L_a\right), \quad (36)$$

$$\mathcal{F}\left(\theta_r; \sigma, L_a\right) = \left[2^{-2c}\times\sum_{j\in\Omega}\sum_{i\in\Omega}\exp\left(-\frac{(i-j)^2}{8\sigma^2\sin^2\theta_r}\right)\right]^{L_a}, \quad (37)$$

where $\mathcal{F}\left(0; \sigma, L_a\right) \triangleq 0$, $L_a = L(n/k - a + 1)$, $b_i = \frac{\theta_r - \theta_{r-1}}{\pi}$, θ_i is arbitrarily chosen with $0 = \theta_0 < \theta_1 < \theta_2 \cdots < \theta_{N-1} < \theta_N = \frac{\pi}{2}$, and N is the maximum subscript of θ_i, which can serve as an flexible accuracy parameter (A detailed explanation of N is given in Example 1).

Example 1. *When $N = 1$, the maximum subscript of θ_i is 1, and we have $\theta_0 = 0$, $\theta_1 = \frac{\pi}{2}$. In addition, we can explicitly calculate*

$$\mathcal{F}\left(\theta_0; \sigma, L_a\right) = 0, \quad b_1 = \frac{1}{2}, \quad (38)$$

$$\mathcal{F}\left(\theta_1; \sigma, L_a\right) = [2^{-2c}\times\sum_{j\in\Omega}\sum_{i\in\Omega}\exp\left(-\frac{(i-j)^2}{8\sigma^2}\right)]^{L_a}. \quad (39)$$

This leads to the closed-form expression:

$$\mathscr{F}_2\left(L_a, \sigma\right) = \frac{1}{2}\cdot\left[2^{-2c}\times\sum_{j\in\Omega}\sum_{i\in\Omega}\exp\left(-\frac{(i-j)^2}{8\sigma^2}\right)\right]^{L_a}. \quad (40)$$

Substituting $\mathscr{F}_2\left(L_a, \sigma\right)$ into (35) leads to an explicit bound.

B. Proof of Theorem 3

The change of the proof initiates with (25). Substitute $y_{i,j} = \text{f}\left(x_{i,j}(\mathbf{M})\right) + n_{i,j}$ into (25), and the probability $\Pr\left(\mathscr{D}(\mathbf{M}') \leq \mathscr{D}(\mathbf{M})\right)$ is reformulated as

$$\Pr\left(\sum_{i=a}^{n/k}\sum_{j=1}^{L}\left[\text{f}\left(\mathbf{x}_{i,j}(\mathbf{M})\right) + n_{i,j} - \text{f}\left(\mathbf{x}_{i,j}(\mathbf{M}')\right)\right]^2 \leq \sum_{i=a}^{n/k}\sum_{j=1}^{L}n_{i,j}^2\right). \quad (41)$$

In what follows we simplify (41) into a vector form.

1) Vector Form of (41)

Define $G_{i,j} \triangleq \text{f}\left(\mathbf{x}_{i,j}(\mathbf{M})\right) - \text{f}\left(\mathbf{x}_{i,j}(\mathbf{M}')\right)$, (41) turns to:

$$\Pr\left(\sum_{i=a}^{n/k}\sum_{j=1}^{L}\left[\underbrace{\text{f}\left(\mathbf{x}_{i,j}(\mathbf{M})\right) - \text{f}\left(\mathbf{x}_{i,j}(\mathbf{M}')\right)}_{G_{i,j}} + n_{i,j}\right]^2 \leq \sum_{i=a}^{n/k}\sum_{j=1}^{L}n_{i,j}^2\right)$$

$$= \Pr\left(\sum_{i=a}^{n/k}\sum_{j=1}^{L}G_{i,j}^2 + 2\sum_{i=a}^{n/k}\sum_{j=1}^{L}G_{i,j}n_{i,j} \leq 0\right). \quad (42)$$

Denote $\mathbf{G}$ as the vector consisted of $\{G_{i,j}\}_{a\leq i\leq[n/k]}^{j\in[L]}$. Since $\mathbf{G}\cdot\mathbf{G}^T = \sum_{i=a}^{n/k}\sum_{j=1}^{L}G_{i,j}^2$ and $\mathbf{G}\cdot[\mathbf{N}^{L_a}]^T = \sum_{i=a}^{n/k}\sum_{j=1}^{L}G_{i,j}n_{i,j}$, the RHS of (42) turns to

$$\Pr\left(\mathbf{G}\left(\mathbf{G} + 2\mathbf{N}^{L_a}\right)^{\text{T}} \leq 0\right). \quad (43)$$

Lemma 2 illustrates the independence between $\mathbf{G}$ and $\mathbf{N}^{L_a}$. Thus, (43) turns to

$$\sum_{\mathbf{g}}\Pr\left(\mathbf{g}\left(\mathbf{g} + 2\mathbf{N}^{L_a}\right)^{\text{T}} \leq 0\right)\cdot\Pr\left(\mathbf{G} = \mathbf{g}\right). \quad (44)$$

2) Closed-Form Solution to (44)

We next show that both $\Pr\left(\mathbf{g}\left(\mathbf{g} + 2\mathbf{N}^{L_a}\right)^{\text{T}} \leq 0\right)$ and $\Pr\left(\mathbf{G} = \mathbf{g}\right)$ can be transformed to a parametric form.

We first analyze $\Pr\left(\mathbf{g}\left(\mathbf{g} + 2\mathbf{N}^{L_a}\right)^{\text{T}} \leq 0\right)$. Fig. 4 indicates that the condition $\mathbf{g}(\mathbf{g} + 2\mathbf{N}^{L_a})^{\text{T}} \leq 0$ is identical to that the projection of $2\mathbf{N}^{L_a}$ onto $\mathbf{g}$, $\text{proj}_{\mathbf{g}}2\mathbf{N}^{L_a}$, is in the opposite direction to the vector $\mathbf{g}$, and $|\text{proj}_{\mathbf{g}}2\mathbf{N}^{L_a}| \geq |\mathbf{g}|$. This insight is formally formulated in the following lemma.
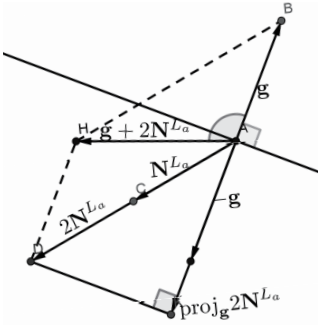
Fig. 4. Geometric relationships among $\mathbf{g}$, $\mathbf{N}^{L_a}$, $\mathbf{g}+2\mathbf{N}^{L_a}$, and $\mathrm{proj}_{\mathbf{g}}2\mathbf{N}^{L_a}$. It is demonstrated that $\mathbf{g}\left(\mathbf{g}+2\mathbf{N}^{L_a}\right)^{\mathrm{T}} \leq 0$ implies that the projection $\mathrm{proj}_{\mathbf{g}}2\mathbf{N}^{L_a}$ is in the opposite direction to the vector $\mathbf{g}$. Additionally, its magnitude satisfies that $|\mathrm{proj}_{\mathbf{g}}2\mathbf{N}^{L_a}| \geq |\mathbf{g}|$.

Lemma 5. *The following equivalence holds true:*

$$\mathbf{g}\left(\mathbf{g}+2\mathbf{N}^{L_a}\right)^{\mathrm{T}} \leq 0 \Leftrightarrow \mathrm{proj}_{\mathbf{g}}2\mathbf{N}^{L_a} = k\mathbf{g}, k \leq -1. \quad (45)$$

Proof. On the one hand, the condition $\mathbf{g}\left(\mathbf{g}+2\mathbf{N}^{L_a}\right)^{\mathrm{T}} \leq 0$ indicates that $\frac{2\mathbf{N}^{L_a}\mathbf{g}^{\mathrm{T}}}{\mathbf{g}\mathbf{g}^{\mathrm{T}}} \leq -1$. On the other hand, we have the definition of the projection $\mathrm{proj}_{\mathbf{g}}2\mathbf{N}^{L_a} \triangleq \frac{2\mathbf{N}^{L_a}\mathbf{g}^{\mathrm{T}}}{\mathbf{g}\mathbf{g}^{\mathrm{T}}} \cdot \mathbf{g}$. Combining these two proposition accomplishes the proof. $\blacksquare$

By applying Lemma 5, we transform the primal condition $\mathbf{g}(\mathbf{g}+2\mathbf{N}^{L_a})^{\mathrm{T}} \leq 0$ on $\mathbf{N}^{L_a}$ into a condition on the projection random vector $\mathrm{proj}_{\mathbf{g}}2\mathbf{N}^{L_a}$: $\mathrm{proj}_{\mathbf{g}}2\mathbf{N}^{L_a} = k\mathbf{g}, k \leq -1$. Because a projection of a Gaussian random vector is another Gaussian random vector, we establish the hypothesis that $\Pr\left(\mathbf{g}(\mathbf{g}+2\mathbf{N}^{L_a})^T \leq 0\right) = Q(\frac{\|\mathbf{g}\|}{2\sigma})$. In the following Lemma, we formally establish this relationship.

Lemma 6. *If $\mathbf{N}^{L_a}$ is a Gaussian random vector, then $\Pr\left(\mathbf{g}(\mathbf{g}+2\mathbf{N}^{L_a})^T \leq 0\right) = Q(\frac{\|\mathbf{g}\|}{2\sigma})$, where $Q(\cdot)$ is the Q function.*

Proof. See Appendix E. $\blacksquare$

Next, we analyze $\Pr\{\mathbf{G}=\mathbf{g}\}$. Because $\mathbf{G} = \mathbf{X}^{L_a}(\mathbf{M}) - \mathbf{X}^{L_a}(\mathbf{M}')$, where $\mathbf{X}^{L_a}(\mathbf{M})$ and $\mathbf{X}^{L_a}(\mathbf{M}')$ is independent with each other (see Appendix C-B), we can apply Lemma 6 and rewrite (44) as:

$$\sum_{\mathbf{i}\in\Omega^{L_a}} \sum_{\mathbf{j}\in\Omega^{L_a}} Q\left(\frac{\|\mathbf{i}-\mathbf{j}\|}{2\sigma}\right) \cdot \Pr\left(\mathbf{X}^{L_a}(\mathbf{M})=\mathbf{i}\right) \cdot \Pr\left(\mathbf{X}^{L_a}(\mathbf{M}')=\mathbf{j}\right),$$
$$(46)$$

where $\mathbf{X}^{L_a}(\mathbf{M})$ and $\mathbf{X}^{L_a}(\mathbf{M}')$ are both uniformly distributed vectors with

$$\Pr\left(\mathbf{X}^{L_a}(\mathbf{M})=\mathbf{i}\right) = 2^{-c\cdot L_a}, \quad (47)$$

$$\Pr\left(\mathbf{X}^{L_a}(\mathbf{M}')=\mathbf{j}\right) = 2^{-c\cdot L_a}. \quad (48)$$

Then, (46) is written in a compact form:

$$\sum_{\mathbf{i}\in\Omega^{L_a}} \sum_{\mathbf{j}\in\Omega^{L_a}} Q\left(\frac{\|\mathbf{i}-\mathbf{j}\|}{2\sigma}\right) \cdot 2^{-2cL_a}. \quad (49)$$

3) Upper Bound (49) *Through Carig's Identity and Rimann Right Sum*

We next establish an explicit upper bound on (49). The core idea is based on Carig's Identity [41] and the Rule of Rimann Right Sum. The Craig's Identity is [41]

$$Q\left(x\right) = \frac{1}{\pi}\int_0^{\frac{\pi}{2}}\exp\left(\frac{-x^2}{2\sin^2\theta}\right)d\theta. \quad (50)$$

Applying (50) in (49) yields

$$\frac{1}{\pi}\int_0^{\frac{\pi}{2}}\left(2^{-2c}\sum_{i\in\Omega}\sum_{j\in\Omega}\exp\left(\frac{-(i-j)^2}{8\sigma^2\sin^2\theta}\right)\right)^{L_a}d\theta. \quad (51)$$

Explicitly solving the integral in (51) is challenging. We instead leverage the *Riemann Sum rule* to establish an explicit upper bound. Denote the integrand in (51) as

$$\mathcal{F}\left(\theta;L_a,\sigma\right) = \left(2^{-2c}\sum_{i\in\Omega}\sum_{j\in\Omega}\exp(\frac{-(i-j)^2}{8\sigma^2\sin^2\theta})\right)^{L_a}. \quad (52)$$

Note that $\mathcal{F}\left(\theta;L_a,\sigma\right)$ satisfies

$$\mathcal{F}\left(0;L_a,\sigma\right) = 0, \frac{d\mathcal{F}\left(\theta;L_a,\sigma\right)}{d\theta} > 0, \text{ for } \forall 0 < \theta < \pi/2. \quad (53)$$

We can apply the *Rule of Right Riemann Sum* to upper bound $\mathcal{F}\left(\theta;L_a,\sigma\right)$. Specifically, we can arbitrarily choose a *partition* of $[0,\frac{\pi}{2}]$, given as $(\theta_0,\theta_1,\cdots,\theta_N)$ such that $0 = \theta_0 < \theta_1 < \theta_2 < \cdots < \theta_{N-1} < \theta_N = \pi/2$ to explicitly upper bound the integral:

$$\frac{1}{\pi}\int_0^{\frac{\pi}{2}}\mathcal{F}\left(\theta;L_a,\sigma\right)d\theta = \sum_{r=1}^N\frac{1}{\pi}\int_{\theta_{r-1}}^{\theta_r}\mathcal{F}\left(\theta;L_a,\sigma\right)d\theta$$
$$\leq \frac{1}{\pi}\sum_{r=1}^N\left(\theta_r-\theta_{r-1}\right)\cdot\mathcal{F}\left(\theta_r;L_a,\sigma\right). \quad (54)$$

Denote $b_r = \frac{\theta_r-\theta_{r-1}}{\pi}$, the RHS of (54) turns to

$$\sum_{r=1}^N b_r\cdot\mathcal{F}\left(\theta_r;L_a,\sigma\right), \quad (55)$$

which is the definition of function $\mathscr{F}_2\left(L_a,\sigma\right)$ given in (36). Then, similar to (33), we have the bound as:

$$\epsilon_a \leq \min\left\{1,\left(2^k-1\right)2^{n-ak}\cdot\mathscr{F}_2\left(L_a,\gamma\right)\right\}. \quad (56)$$

We thus obtain the bound in Theorem 3.

V. APPLICATIONS OF THE BOUND

In this section, we introduce several applications of the bound, providing practical examples to demonstrate insights into effective coding design.

Example 2. *(**Constellation Mapping Design**) One potential applications of the bound is to guide the design of constellation mapping. For Spinal codes, we formulate the following*
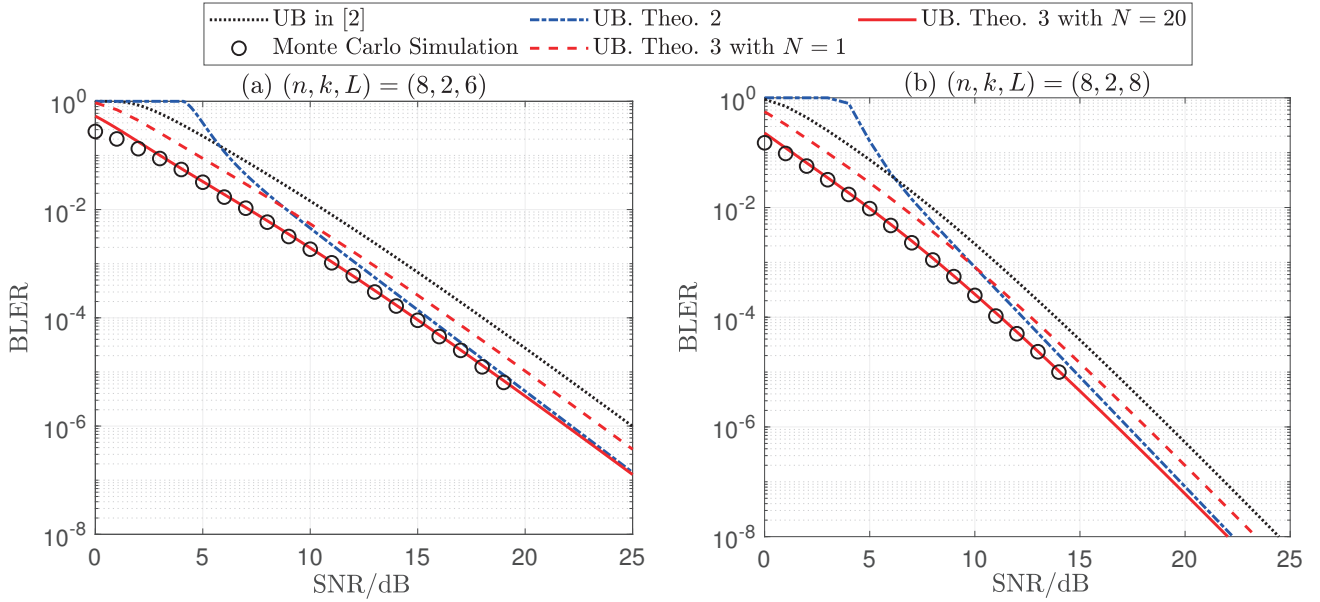
Fig. 5. Comparison of bounds and Monte Carlo simulations. Parameters are set as $n = 8$, $k = 2$, $c = 6$ and $v = 32$.

optimization problem for the constellation mapping design:

$$\min_{\Omega} P_e, \ s.t. \ \mathbb{E}(x^2) \leq P, where \ x \in \Omega, \qquad (57)$$

which minimize the error probability under a power constraint. For a given c, which determines the size of the channel input set Ω as $N = 2^c$, we can rewrite the above problem as

$$\min_{x_1,\cdots,x_N} P_e, \ s.t. \ \frac{1}{N}\sum_{i=1}^{N} x_i^2 \leq P, \qquad (58)$$

where $x_i \in \Omega, i \in \{1, 2, \cdots, N\}$. P_e is difficult to be explicitly solved, so we can minimize the upper bound of P_e instead for the design. Take the bound given in Example 1 as an example, it is easy to verify from (40) that the BLER upper bound minimization problem is equivalent to:

$$\min_{x_1,\cdots,x_N} \sum_{j=1}^{N}\sum_{i=1}^{N} \exp\left(-\frac{(x_i - x_j)^2}{8\sigma^2}\right), \ s.t. \frac{1}{N}\sum_{i=1}^{N} x_i^2 \leq P \qquad (59)$$

We then introduce the Lagrange function $\mathcal{L}(x_1, \cdots, x_N, \lambda)$ for the problem. The Lagrange function is given as

$$\sum_{j=1}^{N}\sum_{i=1}^{N} \exp\left(-\frac{(x_i - x_j)^2}{8\sigma^2}\right) + \frac{\lambda}{N}\sum_{i=1}^{N} x_i^2 - \lambda P. \qquad (60)$$

The problem is equivalent to ensure that

$$\frac{d\mathcal{L}}{d\lambda} = \frac{1}{N}\sum_{i=1}^{N} x_i^2 - P = 0, \qquad (61)$$

$$\frac{d\mathcal{L}}{dx_i} = -\sum_{j=1}^{N} \frac{x_i - x_j}{4\sigma^2} \exp\left(-\frac{(x_i - x_j)^2}{8\sigma^2}\right) + \frac{2\lambda x_i}{N} = 0. \qquad (62)$$

We can then apply the iteration

$$x_i^{(k+1)} = x_i^{(k)} - \alpha\frac{d\mathcal{L}}{dx_i^{(k)}}, i \in \{1, \cdots, N\},$$
$$\lambda^{(k+1)} = \lambda^{(k)} - \beta\frac{d\mathcal{L}}{d\lambda^{(k)}}, \qquad (63)$$

to numerically solve (61), where α and β are predefined step size, and the iteration stops when the gradients are below to a predefined threshold ε with $\frac{d\mathcal{L}}{dx_i^{(k)}} < \varepsilon$ and $\frac{d\mathcal{L}}{d\lambda^{(k)}} < \varepsilon$.

Example 3. *(**Error Floor Prediction**) The BLER analysis enables us to predict the presence of an SNR floor for Spinal codes. This indicates that the BLER will not decrease further, even as the SNR of Spinal codes increases. Specifically, from Theorem 3 we can know that*

$$\lim_{\sigma \to 0} \mathcal{F}(\theta_r; \sigma, L_a) = \left[2^{-2c}\sum_{i=j\in\Omega} \exp\left(-\frac{(i-j)^2}{8\sigma^2 \sin^2\theta_r}\right)\right]^{L_a}$$
$$= \left[2^{-2c} \cdot 2^c\right]^{L_a} = 2^{-cL_a}. \qquad (64)$$

This indicates that an infinitely large SNR does not lead to an arbitrarily small $\mathcal{F}(\theta_r; \sigma, L_a)$, and thus does not lead to an arbitrarily small BLER. This phenomenon is called error floor in coding theory. Furthermore, we can know from (64) and $L_a = L(n/k - a + 1)$ that an increase of c, n/k, or L will decrease the error floor of Spinal codes.

VI. SIMULATION RESULTS AND DISCUSSIONS

In this section, we employ Monte Carlo simulations to validate the accuracy of our derived bound. In addition, we theoretically establish that our proposed bounds are tighter than previous results in [2].
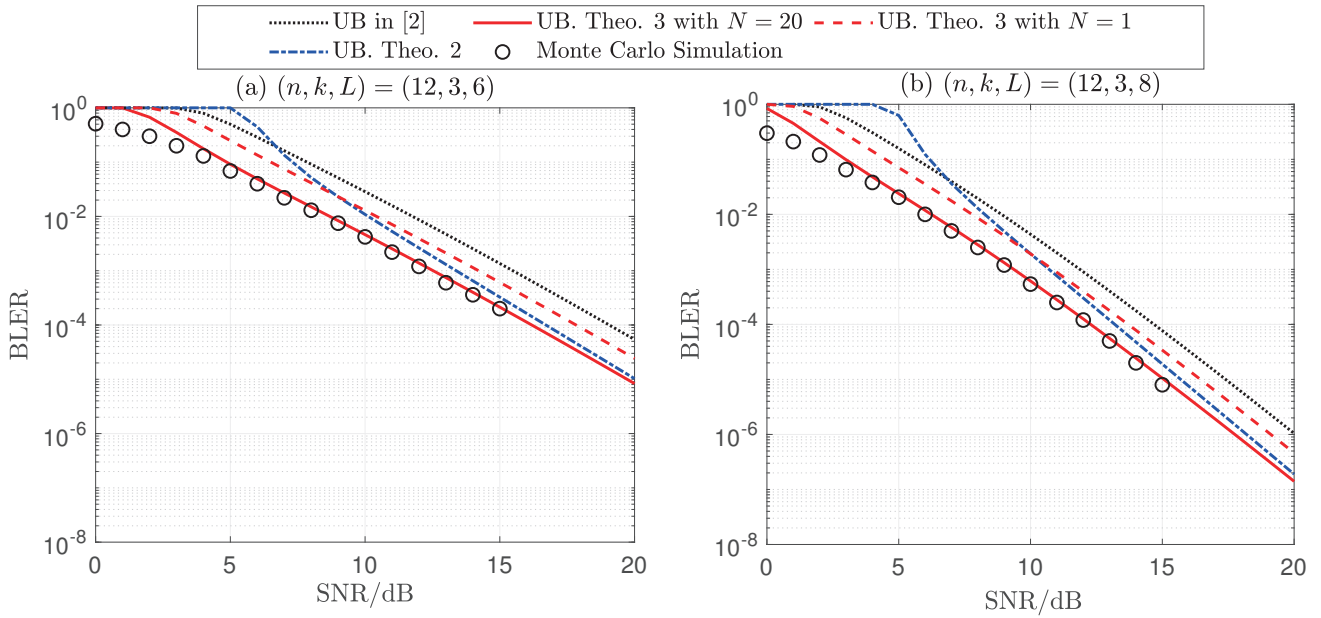
Fig. 6. Comparison of bounds and Monte Carlo simulations. Parameters are set as $n = 12$, $k = 3$, $c = 6$ and $v = 32$.

A. Observations and Verification

Fig. 5 and Fig. 6 illustrate the bound in [2], the developed Theorem 2 and Theorem 3 in this paper, and Monte Carlo simulation results. Due to the exponential complexity of ML-decoding in terms of n, we select $(n, k) = (8, 2)$ and $(n, k) = (12, 3)$ here for a feasible simulation to verify our theoretical results. Fig. 5 compares the results under $(n, k) = (8, 2)$, and Fig. 6 is under $(n, k) = (12, 3)$. The Monte Carlo simulations are conducted to approximate the average error probability, where $c = 6$ and $v = 32$ are chosen to verify our theoretical results[3]. The number of transmitted passes is set as $L = 6$ and $L = 8$ for the simulation setup[4].

From Fig. 5 and Fig. 6, we can obtain two insights: (i) Our proposed Theorem 2 yields tighter approximations in high-SNR scenarios compared to the bound in [2]. The reasons for this phenomenon are shown in Fig. 3: When the encoded symbol vector $\mathbf{X}^{L_a}(\mathbf{M})$ is close to the hypercube's boundary, bounding the intersection volume as the hypersphere volume can be overestimated especially when $|\mathbf{N}^{L_a}|$ is large. Hence, the upper bound in (28) tends to 1 under low SNR, and demonstrates tight approximations under high SNR; (ii) Our derived Theorem 3 maintains its tightness over a wide range of SNR. This is because Theorem 3 addresses the difficulty in approximating BLER under low-SNR by considering the randomness of $\mathbf{X}^{L_a}(\mathbf{M})$. In addition, by choosing $N = 20$, the Rule of Riemann Right Sum can accurately approximate the integral in (51). Our derived bounds achieve uniform tightness under a wide range of SNR and different parameter setup.

Fig. 7 demonstrates the convergence curve and BLER comparisons among the constellation mapping designs. The

left panel is the convergence curve of our proposed iteration algorithm. It shows that the proposed algorithm is able to achieve zero gradient of the *Lagrange function* $\mathcal{L}$, which successfully solves the constellation mapping design under power constraints. The right panel compares our proposed constellation mapping design with two benchmark constellation mappings of Spinal codes:

- *Uniform*: the channel input set is established by [5, Section 3.3], given as

$$\Omega = \left\{ \frac{b + \frac{1}{2}}{2^c} - \frac{1}{2} : b = 0, 1, \cdots, 2^c - 1 \right\}. \quad (65)$$

- *Truncated Gaussian*: the channel input set is established by [5, Section 3.3], given as

$$\Omega = \left\{ \Phi^{-1} \left(\beta + \frac{(1 - 2\beta)(b + \frac{1}{2})}{2^c} \right) : b = 0, \cdots, 2^c - 1 \right\}. \quad (66)$$

It is demonstrated that the *uniform* constellation achieves better BLER performance under high SNR regime, whereas the *truncated Gaussian* constellation achieves better BLER performance under low SNR regime. Our proposed constellation mapping scheme, termed as "Optimal" in the figure, achieves the best BLER performance over the wide range of BLER.

B. Theoretical Implications

It has been observed from the previous subsection that the proposed Theorem 3 achieves uniform tightness over a wide range of SNR. This subsection delves into the theoretical implication to explore why our proposed result Theorem 3 achieves greater tightness compared to the result resorting to the 1965 *Gallager random coding bound* [2].

In what follows we theoretically establish the tightness of Theorem 3 in two steps. First, we prove that the bound when
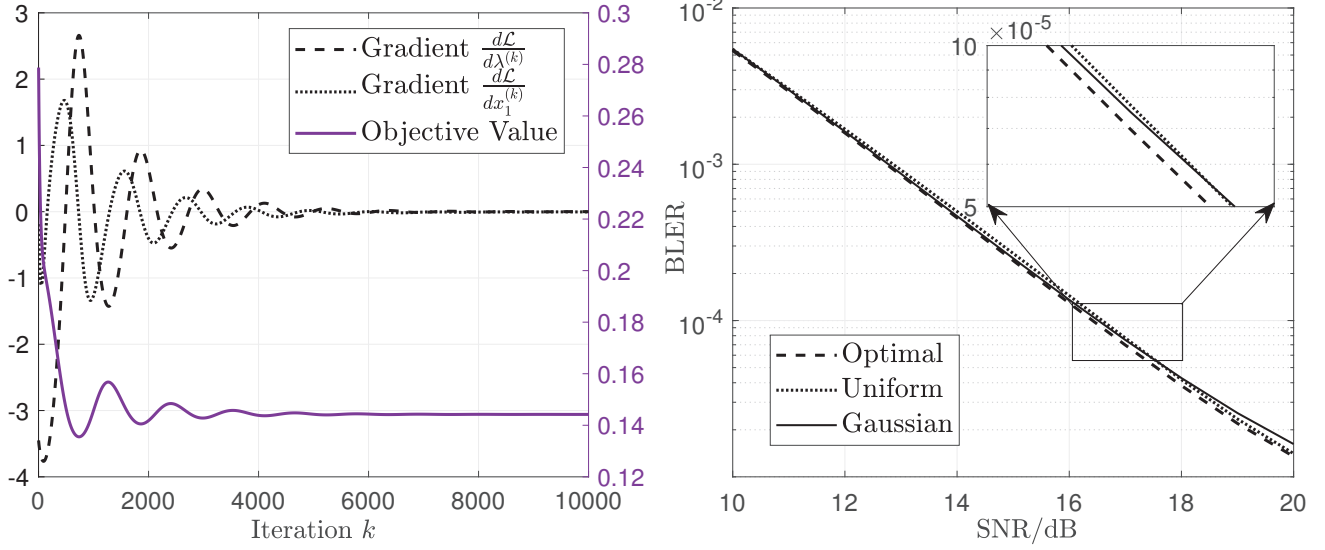
---

[3]This is a general parameter setup for Spinal codes [5].

[4]Different parameters are chosen to verify the robustness of the derived bounds.

Fig. 7. Convergence curve and BLER comparisons of the constellation mapping designs. Parameters are set as $n = 8$, $c = 6$, $v = 32$, $k = 2$.

$N = 1$, as shown in Example 1, is the most relaxed version of the bound in Theorem 3. This is formulated in the following Lemma.

Lemma 7. *For any N, $0 = \theta_0 \leq \theta_1, \cdots, \theta_{N-1} \leq \theta_N = \pi/2$, the parameter setup with $N = 1$ is the most relaxed bound of Theorem 3.*

Proof. From (53) we know that for any $\theta_r \leq \theta_N$, $\mathcal{F}(\theta_r; L_a, \sigma) \leq \mathcal{F}(\theta_r; L_a, \sigma)$. Substituting this inequality into the RHS of (54) yields that, for any $\theta_r, 0 \leq r \leq N$,

$$\frac{1}{\pi} \sum_{r=1}^{N} (\theta_r - \theta_{r-1}) \cdot \mathcal{F}(\theta_r; L_a, \sigma) \leq \frac{\theta_N}{\pi} \cdot \mathcal{F}(\theta_N; L_a, \sigma)$$
$$= \frac{1}{2} \cdot \mathcal{F}\left(\frac{\pi}{2}; L_a, \sigma\right) \quad (67)$$

Because the RHS of (67) is equal to the RHS of (36) when $N = 1$, we thus accomplish the proof. ∎

Then, we prove that even the worst case of Theorem 3 is tighter than the bound presented in Theorem 1. Denote the bound on $\Pr\left\{\mathcal{E}_a \left| \bigcap_{j=1}^{a-1} \bar{\mathcal{E}}_j \right.\right\}$ in Theorem 1 as $\bar{\epsilon}_a$ and the bound in Example 1 as $\bar{\bar{\epsilon}}_a$. We establish the following lemma.

Lemma 8. *The inequality $\bar{\bar{\epsilon}}_a < \bar{\epsilon}_a$ holds true.*

Proof. Substituting the simplified $E_0(Q)$ in (13) into (8), we rewrite $\bar{\epsilon}_a$ as

$$\bar{\epsilon}_a = 2^{k(n/k-a+1)} \cdot \left(2^{-2c} \times \sum_{j \in \Omega} \sum_{i \in \Omega} \exp\left(-\frac{(i-j)^2}{8\sigma^2}\right)\right)^{L_a} . \quad (68)$$

In Example 1, it has been derived that $\mathcal{F}_2(L_a, \sigma) = \frac{1}{2} \cdot \left[2^{-2c} \times \sum_{j \in \Omega} \sum_{i \in \Omega} \exp\left(-\frac{(i-j)^2}{8\sigma^2}\right)\right]^{L_a}$. Consequently, $\bar{\epsilon}_a$ can be simplified as $2^{k(n/k-a+1)+1} \cdot \mathcal{F}_2(L_a, \sigma)$. $\bar{\bar{\epsilon}}_a$ is given

as $\min\left\{1, \left(2^k - 1\right) 2^{n-ak} \cdot \mathcal{F}_2(L_a, \sigma)\right\}$. This indicates that $\bar{\bar{\epsilon}}_a \leq \left(2^k - 1\right) 2^{n-ak} \cdot \mathcal{F}_2(L_a, \sigma)$. Subtract $\bar{\bar{\epsilon}}_a$ from $\bar{\epsilon}_a$, and we have that

$$\bar{\epsilon}_a - \bar{\bar{\epsilon}}_a \geq (2^{k(n/k-a+1)+1} - \left(2^k - 1\right) 2^{n-ak}) \cdot \mathcal{F}_2(L_a, \sigma)$$
$$= 2^{n-ak} \cdot (2^{k+1} - 2^k + 1) \cdot \mathcal{F}_2(L_a, \sigma)$$
$$= 2^{n-ak} \cdot (2^k + 1) \cdot \mathcal{F}_2(L_a, \sigma) > 0. \quad (69)$$

Thus we establish that $\bar{\bar{\epsilon}}_a < \bar{\epsilon}_a$. ∎

Additionally, Fig. 5 demonstrates that our proposed bound in Theorem 2 is tighter than the bound in [2] under high-SNR regime. Subsequently, we reveal this relationship by discussing the asymptotic tightness of our proposed bound given in Theorem 2. Denote the bound in Theorem 1 as $P_e^{(1)}$ and that in 2 as $P_e^{(2)}$. We establish the following lemma.

Lemma 9. *The following asymptotic inequality hold true:*

$$\lim_{\gamma \to \infty} P_e^{(2)} < \lim_{\gamma \to \infty} P_e^{(1)}. \quad (70)$$

Proof. See Appendix F. ∎

VII. CONCLUSIONS

This paper has established a new probability framework to analyze the upper bound on the BLER of ML-decoded Spinal codes over the AWGN channel. Different from the conventional reliance on the 1965 *Gallager random coding bound*, which might not fully account for the unique attributes of Spinal codes, we have developed new methods to refine the analysis. The main results of this paper are two tighter upper bounds on the BLER of Spinal codes. These bounds have been validated through simulations, and their improved tightness has been proved. We have also discussed potential applications of the bounds that may provide insights for the coding design.

Our findings may also highlight several avenues for future research. Notably, our error analysis presumes a sufficiently

large v, neglecting potential hash collisions. Future work could focus on exploring the balance between coding-decoding complexity and error probability with respect to v, aiding in the efficient design of hash functions. Furthermore, applying these tighter bounds to develop other high-efficiency coding strategies, such as unequal error protection and concatenation with outer codes, is an exciting research direction.

APPENDIX A
PROOF OF COROLLARY 1

The corollary is proved through an expansion of $\Pr\{h(\mathbf{s}, \mathbf{m}) = h(\mathbf{s}', \mathbf{m}')\}$ and the adoption of Lemma 1:

$$
\begin{aligned}
&\Pr\{h(\mathbf{s}, \mathbf{m}) = h(\mathbf{s}', \mathbf{m}')\} \\
&= \sum_{\mathbf{x} \in \{0,1\}^v} \underbrace{\Pr\{h(\mathbf{s}, \mathbf{m}) = \mathbf{x}, h(\mathbf{s}', \mathbf{m}') = \mathbf{x}\}}_{2^{-2v}} \quad (71) \\
&= 2^v \cdot 2^{-2v} = 2^{-v}.
\end{aligned}
$$

APPENDIX B
AN APPROACH TO CALCULATE $E_0(\mathcal{Q})$

For our considered Spinal codes, the channel input set is $\Omega = \{0, 1, 2, \cdots, 2^c - 1\}$, wherein each coded symbol follows the uniform distribution with $\mathcal{Q}(x) = 2^{-c}$. Applying this in (9), and we simplify the form of $E_0(\mathcal{Q})$ as

$$
\begin{aligned}
&-\ln\left\{\frac{1}{\sqrt{2\pi\sigma^2}}\int_{\mathbb{R}}\left(\sum_{i\in\Omega}2^{-c}\cdot\exp\left(-\frac{(y-i)^2}{4\sigma^2}\right)\right)^2 dy\right\} \\
&= -\ln\left\{\frac{2^{-2c}}{\sqrt{2\pi\sigma^2}}\int_{\mathbb{R}}\left(\sum_{i,j\in\Omega}\exp\left(-\frac{(y-i)^2+(y-j)^2}{4\sigma^2}\right)\right)dy\right\} \\
&= -\ln\left\{\frac{2^{-2c}}{\sqrt{2\pi\sigma^2}}\sum_{j,i\in\Omega}\exp\left(-\frac{(i-j)^2}{8\sigma^2}\right)\int_{\mathbb{R}}\exp\left(-\frac{\left(y-\frac{i+j}{2}\right)^2}{2\sigma^2}\right)dy\right\} \\
&= -\ln\left\{2^{-2c}\sum_{j\in\Omega}\sum_{i\in\Omega}\exp\left(-\frac{(i-j)^2}{8\sigma^2}\right)\right\}. \quad (72)
\end{aligned}
$$

APPENDIX C
PROOF OF LEMMA 2

A. Proof of Assertion (i)

First, we establish the following Lemma:

Lemma 10. *If $\forall 1 \le i < a, \mathbf{m}_i = \mathbf{m}'_i$, then $\forall 1 \le i < a, \mathbf{s}_i = \mathbf{s}'_i$.*

Proof. We conduct the mathematical induction:
(1) We validate that $\mathbf{s}_0 = \mathbf{s}'_0$. Since $\mathbf{s}_0$ is pre-shared across the transmitter and the receiver as $\mathbf{s}_0 = \mathbf{s}'_0 = \mathbf{0}^v$, this validation is obvious.
(2) We hypothesis that $\mathbf{s}_{i-1} = \mathbf{s}'_{i-1}$ is true, and prove $\forall 1 \le i < a, \mathbf{s}_i = \mathbf{s}'_i$. The proof involves revisiting the hash function:

$$
\mathbf{s}_i = h(\mathbf{m}_i, \mathbf{s}_{i-1}) = h(\mathbf{m}'_i, \mathbf{s}'_{i-1}) = \mathbf{s}'_i, \quad (73)
$$

where $\mathbf{m}_i = \mathbf{m}'_i$ is the condition and $\mathbf{s}_{i-1} = \mathbf{s}'_{i-1}$ is the hypothesis. ∎

Lemma 10 points out that the seeds of the RNGs are the same as $\forall 1 \le i < a, \mathbf{s}_i = \mathbf{s}'_i$. In this way, the coded pseudo-random symbols generated by the RNG seeded with $\mathbf{s}_i$ are the same as those generated by the RNG seeded with $\mathbf{s}'_i$, satisfying that $\forall 1 \le i < a, \mathrm{f}(\mathbf{x}_{i,j}(\mathbf{M}')) = \mathrm{f}(\mathbf{x}_{i,j}(\mathbf{M}))$.

As such, we have $\forall 1 \le i < a, y_{i,j} - \mathrm{f}(\mathbf{x}_{i,j}(\mathbf{M}')))^2 = y_{i,j} - \mathrm{f}(\mathbf{x}_{i,j}(\mathbf{M})))^2 = n_{i,j}^2$.

B. Proof of Assertion (ii)

We first establish the following Lemma:

Lemma 11. *If $\mathbf{m}_a \ne \mathbf{m}'_a$, then $\forall a \le i \le n/k, \Pr\{\mathbf{s}_i = \mathbf{s}'_i\} \le 1 - (1 - 2^{-v})^{i-a+1}$.*

Proof. Denote E_i as the event that $\bigcap_{j=a}^{i} \mathbf{s}_j \ne \mathbf{s}'_j$, then by leveraging corollary 1, we have $\forall a \le i \le n/k, \Pr(E_{i+1}|E_i) = 1 - 2^{-v}$. Therefore, since $E_i \subset E_{i-1}$,

$$
\begin{aligned}
\Pr(E_i) &= \Pr\left(E_i \bigcap E_{i-1}\right) = \Pr(E_i|E_{i-1})\Pr(E_{i-1}) \\
&= (1 - 2^{-v})\Pr(E_{i-1}) = (1 - 2^{-v})^2\Pr(E_{i-2}) \\
&= \cdots \\
&= (1 - 2^{-v})^{i-a+1}.
\end{aligned}
$$
$$(74)$$

Since $\Pr(E_{i-1}) = (1 - 2^{-v})^{i-a}$ and $\Pr(\mathbf{s}_i = \mathbf{s}'_i|E_{i-1}) = 2^{-v}$ we then establish the inequality between $\Pr\{\mathbf{s}_i = \mathbf{s}'_i\}$ and $\Pr\{\mathbf{s}_{i-1} = \mathbf{s}'_{i-1}\}$ leveraging the *union bound*:

$$
\begin{aligned}
\Pr\{\mathbf{s}_i = \mathbf{s}'_i\} &= \Pr(E_{i-1}, \mathbf{s}_i = \mathbf{s}'_i) + \Pr(\overline{E_{i-1}}, \mathbf{s}_i = \mathbf{s}'_i) \\
&\le \Pr(E_{i-1})\Pr(\mathbf{s}_i = \mathbf{s}'_i|E_{i-1}) + \Pr(\mathbf{s}_{i-1} = \mathbf{s}'_{i-1}, \mathbf{s}_i = \mathbf{s}'_i) \\
&\le (1 - 2^{-v})^{i-a} \cdot 2^{-v} + \Pr(\mathbf{s}_{i-1} = \mathbf{s}'_{i-1}).
\end{aligned}
$$
$$(75)$$

Iterating (75) yields the inequality $\Pr\{\mathbf{s}_i = \mathbf{s}'_i\} \le \sum_{j=a}^{i}(1 - 2^{-v})^{j-a} \cdot 2^{-v} = 1 - (1 - 2^{-v})^{i-a+1}$. ∎

With Lemma 11, we then adopt the sandwich theorem, and have that

$$
0 \le \lim_{v\to\infty}\Pr\{\mathbf{s}_i = \mathbf{s}'_i\} \le \lim_{v\to\infty} 1 - (1 - 2^{-v})^{i-a+1} = 0. \quad (76)
$$

Consequently, it follows that $\lim_{v\to\infty}\Pr(\mathbf{s}_i = \mathbf{s}'_i) = 0$. This implies that as the parameter v grows, the probability of event $\mathbf{s}_i = \mathbf{s}'_i$ becomes negligible. In this case, we can assert $\forall a \le i \le n/k, \mathbf{s}_i \ne \mathbf{s}'_i$ when confronted with a sufficiently large v, which then leads to $\forall a \le i \le n/k, \mathrm{f}(\mathbf{x}_{i,j}(\mathbf{M}'))$ is independent with $\mathrm{f}(\mathbf{x}_{i,j}(\mathbf{M}))$. Note that $\mathrm{f}(\mathbf{x}_{i,j}(\mathbf{M}'))$ is independent with $n_{i,j}$ and $y_{i,j} = \mathrm{f}(\mathbf{x}_{i,j}(\mathbf{M})) + n_{i,j}$, as desired, we complete the proof of assertion (ii).

APPENDIX D
PROOF OF LEMMA 4

We first transform the RHS of (31) as a piece-wise function. Let

$$
\frac{\left(\pi \sum_{i=a}^{n/k}\sum_{j=1}^{L} n_{i,j}^2\right)^{L_a/2}}{(2^c - 1)^{L_a}\Gamma\left(1 + \frac{L_a}{2}\right)} = 1, \quad (77)
$$

we have

$$
\sqrt{\sum_{i=a}^{n/k}\sum_{j=1}^{L} n_{i,j}^2} = \frac{(2^c - 1)\Gamma(1 + L_a/2)^{1/L_a}}{\sqrt{\pi}}. \quad (78)
$$

$$\underbrace{\frac{1}{\left(\sqrt{2\pi\sigma^2}\right)^{L_a}} \int \cdots \int_{\sum_{i=a}^{n/k} \sum_{j=1}^{L} n_{i,j}^2 \leq \mathcal{D}^2} \frac{\left(\pi \sum_{i=a}^{n/k} \sum_{j=1}^{L} n_{i,j}^2\right)^{L_a/2}}{(2^c-1)^{L_a}\Gamma\left(1+\frac{L_a}{2}\right)} e^{-\frac{\sum_{i=a}^{n/k}\sum_{j=1}^{L} n_{i,j}^2}{2\sigma^2}} \prod_{i=a}^{n/k} \prod_{j=1}^{L} dn_{i,j}}_{\mathcal{J}_1} + \underbrace{\frac{1}{\left(\sqrt{2\pi\sigma^2}\right)^{L_a}} \int \cdots \int_{\sum_{i=a}^{n/k} \sum_{j=1}^{L} n_{i,j}^2 \geq \mathcal{D}^2} e^{-\frac{\sum_{i=a}^{n/k}\sum_{j=1}^{L} n_{i,j}^2}{2\sigma^2}} \prod_{i=a}^{n/k} \prod_{j=1}^{L} dn_{i,j}}_{\mathcal{J}_2}.$$

$$(80)$$

$$\mathcal{J}_1 = \frac{\int_0^{\mathcal{D}} r^{2L_a-1} e^{\frac{-r^2}{2\sigma^2}} dr}{\left(\sqrt{2\sigma^2}\right)^{L_a} (2^c-1)^{L_a}\Gamma\left(1+\frac{L_a}{2}\right)} \int_0^{2\pi} \int_0^{\pi} \cdots \int_0^{\pi} \left(\prod_{i=1}^{L_a-2} \sin^{L_a-1-i}(\phi_i) d\phi_i\right) d\phi_{L_a-1},$$

$$\mathcal{J}_2 = \frac{\int_{\mathcal{D}}^{\infty} r^{L_a-1} e^{\frac{-r^2}{2\sigma^2}} dr}{\left(\sqrt{2\sigma^2}\right)^{L_a}} \int_0^{2\pi} \int_0^{\pi} \cdots \int_0^{\pi} \left(\prod_{i=1}^{L_a-2} \sin^{L_a-1-i}(\phi_i) d\phi_i\right) d\phi_{L_a-1},$$

$$(83)$$

Let $\mathcal{D} = \frac{(2^c-1)\Gamma(1+L_a/2)^{1/L_a}}{\sqrt{\pi}}$, the integrand of (31) is expressed as a piece-wise function:

$$\min\left\{1, \frac{\left(\pi \sum_{i=a}^{n/k} \sum_{j=1}^{L} n_{i,j}^2\right)^{L_a/2}}{(2^c-1)^{L_a}\Gamma\left(1+\frac{L_a}{2}\right)}\right\} =$$

$$\begin{cases} 1 & \text{if } \sqrt{\sum_{i=a}^{n/k} \sum_{j=1}^{L} n_{i,j}^2} \geq \mathcal{D}, \\ \frac{\left(\pi \sum_{i=a}^{n/k} \sum_{j=1}^{L} n_{i,j}^2\right)^{L_a/2}}{(2^c-1)^{L_a}\Gamma\left(1+\frac{L_a}{2}\right)} & \text{if } \sqrt{\sum_{i=a}^{n/k} \sum_{j=1}^{L} n_{i,j}^2} < \mathcal{D}. \end{cases}$$

$$(79)$$

Plug the piece-wise function (79) in the L_a-dimension integral in (31), the integral turns to (80) at the top of this page. We define $\mathcal{J}_1$ as the first term and $\mathcal{J}_2$ as the second term on the RHS of (80). To solve both $\mathcal{J}_1$ and $\mathcal{J}_2$, we propose a method of variable substitution to simplify the integration process. Specifically, this involves transitioning from *Cartesian coordinates* $(n_{a,1}, \cdots, n_{n/k,L})$ to *hyperspherical coordinates* $(r, \phi_1, \cdots, \phi_{L_a-1})$:

$$n_{a,1} = r\cos\phi_1,$$
$$n_{a,2} = r\sin\phi_1\cos\phi_2,$$
$$\vdots$$
$$n_{n/k,L-1} = r\sin\phi_1\cdots\sin\phi_{L_a-2}\cos\phi_{L_a-1},$$
$$n_{n/k,L} = r\sin\phi_1\cdots\sin\phi_{L_a-2}\sin\phi_{L_a-1}.$$

$$(81)$$

The *Jacobian determinant* plays a crucial role when performing variable substitution in integral transformations. In the context of our analysis, the *Jacobian determinant* can be calculated as:

$$\det\left(\frac{\partial n_{i,j}}{\partial(r,\phi_\kappa)}\right) = r^{L_a-1} \prod_{i=1}^{L_a-2} \sin^{L_a-1-i}(\phi_i), \qquad (82)$$

Now, we can rewrite $\mathcal{J}_1$ and $\mathcal{J}_2$ as given in (83) at the top of this page, where the multiple integrals on the RHS is:

$$\int_0^{2\pi}\int_0^{\pi}\cdots\int_0^{\pi}\left(\prod_{i=1}^{L_a-2}\sin^{L_a-1-i}(\phi_i)d\phi_i\right)d\phi_{L_a-1} = \frac{\pi^{L_a/2}L_a}{\Gamma\left(1+\frac{L_a}{2}\right)}.$$

$$(84)$$

Then, substituting (84) into (83) yields

$$\frac{\pi^{L_a/2}L_a \int_0^{\mathcal{D}} r^{2L_a-1}e^{-\frac{r^2}{2\sigma^2}}dr}{(2^c-1)^{L_a}\Gamma^2\left(1+\frac{L_a}{2}\right)\left(\sqrt{2\sigma^2}\right)^{L_a}} + \frac{L_a\int_{\mathcal{D}}^{\infty} r^{L_a-1}e^{-\frac{r^2}{2\sigma^2}}dr}{\Gamma\left(1+\frac{L_a}{2}\right)\left(\sqrt{2\sigma^2}\right)^{L_a}},$$

$$(85)$$

where $\int_0^{\mathcal{D}} r^{2L_a-1}e^{-\frac{r^2}{2\sigma^2}}dr$ and $\int_{\mathcal{D}}^{\infty} r^{L_a-1}e^{-\frac{r^2}{2\sigma^2}}dr$ can be explicitly expressed in Lemma 12 and Lemma 13, respectively, with $\mathcal{D} = \frac{(2^c-1)\Gamma(1+L_a/2)^{1/L_a}}{\sqrt{\pi}}$.

Lemma 12. $\int_0^{\mathcal{D}} r^{2L_a-1}e^{-\frac{r^2}{2\sigma^2}}dr$ *is explicit, given as:*

$$\sigma^{2L_a}\left(-e^{\frac{-\mathcal{D}^2}{2\sigma^2}}\sum_{i=1}^{L_a}\frac{\mathcal{D}^{2(L_a-i)}}{\sigma^{2(L_a-i)}}\mathcal{I}_{i-1} + \mathcal{I}_{L_a-1}\right), \qquad (86)$$

where $\mathcal{I}_i \triangleq \prod_{j=1}^{i} 2(L_a-j)$.

Proof. See Appendix G. ∎

Lemma 13. $\int_{\mathcal{D}}^{\infty} r^{L_a-1}e^{-\frac{r^2}{2\sigma^2}}dr$ *is explicit, given as::*

$$\begin{cases} \sigma^{L_a}e^{\frac{-\mathcal{D}^2}{2\sigma^2}}G(L_a/2), & L_a \text{ is even} \\ \sigma^{L_a}\left(\sqrt{2\pi}Q\left(\frac{\mathcal{D}}{\sigma}\right)\mathcal{K}_{\frac{(L_a-3)}{2}} + e^{\frac{-\mathcal{D}^2}{2\sigma^2}}G\left(\frac{L_a-1}{2}\right)\right), & L_a \text{ is odd} \end{cases},$$

$$(87)$$

where $\mathcal{K}_i \triangleq \prod_{j=1}^{i}(L_a-2j)$ *and* $G(x) = \sum_{i=1}^{x}\frac{\mathcal{D}^{L_a-2i}}{\sigma^{L_a-2i}}\cdot\mathcal{K}_{i-1}$.

Proof. See Appendix H. ∎

By applying Lemma 12 and Lemma 13 in Lemma 4, we derive the explicit expression for the L_a-dimension integral in (31). Our remaining focus is to restructure the RHS of (85) for

better tractability in terms of SNR γ. For uniformly distributed Spinal codes, the SNR γ can be approximated as

$$\gamma = \frac{\mathbb{E}\,f(\mathbf{x}_{i,j}(\mathbf{M}'))}{\sigma^2} = \frac{(2^c-1)^2-1}{12\sigma^2} \approx \frac{(2^c-1)^2}{12\sigma^2}. \quad (88)$$

From the deduction $\frac{2^c-1}{\sigma} = \sqrt{12\gamma}$, we are able to recast $\frac{\mathcal{D}}{\sigma}$ in a form that is reliant on γ:

$$\frac{\mathcal{D}}{\sigma} = \frac{(2^c-1)\,\Gamma(1+L_a/2)^{1/L_a}}{\sigma\sqrt{\pi}} = \sqrt{\frac{12\gamma}{\pi}}\Gamma(1+L_a/2)^{1/L_a}. \quad (89)$$

Denote the RHS of (89) as $\beta(L_a,\gamma)$ and substitute it into (86), the integral $\int_0^{\mathcal{D}} r^{2L_a-1}e^{-\frac{r^2}{2\sigma^2}}\,dr$ turns to

$$\sigma^{2L_a}\left(-e^{\frac{-\beta(L_a,\gamma)^2}{2}}\sum_{i=1}^{L_a}\beta(L_a,\gamma)^{2(L_a-i)}\mathcal{I}_{i-1} + \mathcal{I}_{L_a-1}\right). \quad (90)$$

Similarly, substituting $\frac{\mathcal{D}}{\sigma} = \beta(L_a,\gamma)$ into (87) and the integral $\int_{\mathcal{D}}^{\infty} r^{L_a-1}e^{-\frac{r^2}{2\sigma^2}}\,dr$ turns to (18).

Define $\mathscr{H}(L_a,\gamma) \triangleq \int_{\mathcal{D}}^{\infty} r^{2L_a-1}e^{-\frac{r^2}{2\sigma^2}}\,dr/\sigma^{2L_a}$, and $\mathscr{G}(L_a,\gamma) \triangleq \int_{\mathcal{D}}^{\infty} r^{L_a-1}e^{-\frac{r^2}{2\sigma^2}}\,dr/\sigma^{L_a}$, we explicitly express $\mathscr{G}(L_a,\gamma)$ and $\mathscr{H}(L_a,\gamma)$ as given in (17) and (18). Then, substituting (17) and (18) into (85) accomplishes the proof.

APPENDIX E
PROOF OF LEMMA 6

To rigorously prove this, we introduce a rotation matrix that operates within the L_a-dimension hyperspace. The L_a-dimension rotation matrix is given as $\mathbf{A}$, with

$$\mathbf{A} = \begin{bmatrix}\mathbf{A}_1 \\ \vdots \\ \mathbf{A}_{L_a}\end{bmatrix} \in \mathbb{R}^{L_a \times L_a}, \quad \mathbf{A}\mathbf{g}^{\mathrm{T}} = \begin{bmatrix}\|\mathbf{g}\|, \underbrace{0,\cdots,0}_{L_a-1}\end{bmatrix}^{\mathrm{T}}. \quad (91)$$

The second term of (91) is formulated to ensure that the rotation matrix $\mathbf{A}$ rotates the vector $\mathbf{g}$ along an axis, thereby simplifying the analysis. Being a rotation matrix, $\mathbf{A}$ fulfills that $\mathbf{A}^{\mathrm{T}}\mathbf{A} = \mathbf{I}_{L_a}$. This property helps simplify the probability

$$\Pr\left(\mathbf{g}\left(\mathbf{g}+2\mathbf{N}^{L_a}\right)^{\mathrm{T}} \le 0\right)$$
$$= \Pr\left(\mathbf{g}\mathbf{A}^{\mathrm{T}}\mathbf{A}\left(\mathbf{g}+2\mathbf{N}^{L_a}\right)^{\mathrm{T}} \le 0\right) \quad (92)$$
$$= \Pr\left(\left[\mathbf{A}\mathbf{g}^{\mathrm{T}}\right]^{\mathrm{T}}\left(\mathbf{A}\mathbf{g}^{\mathrm{T}}+2\mathbf{A}\left[\mathbf{N}^{L_a}\right]^{\mathrm{T}}\right) \le 0\right).$$

Substituting the second term of (91) into the RHS of (92) yields

$$\Pr\left(\left[\mathbf{A}\mathbf{g}^{\mathrm{T}}\right]^{\mathrm{T}}\left(\mathbf{A}\mathbf{g}^{\mathrm{T}}+2\mathbf{A}\left[\mathbf{N}^{L_a}\right]^{\mathrm{T}}\right) \le 0\right)$$
$$= \Pr\left(\|\mathbf{g}\|^2 + 2\|\mathbf{g}\| \cdot \mathbf{A}_1\left[\mathbf{N}^{L_a}\right]^{\mathrm{T}} \le 0\right)$$
$$= \Pr\left(\mathbf{A}_1\left[\mathbf{N}^{L_a}\right]^{\mathrm{T}} \le -\frac{\|\mathbf{g}\|}{2}\right), \quad (93)$$

which can be expanded as an L_a-fold integral

$$\overbrace{\int\cdots\int}^{L_a}_{\mathbf{A}_1[\mathbf{N}^{L_a}]^{\mathrm{T}} \le -\frac{\|\mathbf{g}\|}{2}} \frac{1}{\left(\sqrt{2\pi\sigma^2}\right)^{L_a}}e^{-\frac{\|\mathbf{N}^{L_a}\|^2}{2\sigma^2}}\prod_{i=a}^{n/k}\prod_{j=1}^{L}dn_{i,j}. \quad (94)$$

The complexity of (94) arises from the abstract nature of the integration region $\mathbf{A}_1\left[\mathbf{N}^{L_a}\right]^{\mathrm{T}} \le -\frac{\|\mathbf{g}\|}{2}$. To simplify this integration region, we introduce an additional rotation matrix $\mathbf{B}$. The rotation matrix is defined as

$$\mathbf{B} \triangleq \begin{bmatrix}\mathbf{B}_1 \\ \vdots \\ \mathbf{B}_{L_a}\end{bmatrix} \in \mathbb{R}^{L_a \times L_a}, \quad (95)$$

which should satisfy that $\mathbf{B}\mathbf{B}^{\mathrm{T}} = \mathbf{I}_{L_a}$ and

$$\mathbf{B}\left[\mathbf{N}^{L_a}\right]^{\mathrm{T}} = \begin{bmatrix}\mathbf{A}_1\left[\mathbf{N}^{L_a}\right]^{\mathrm{T}}, \underbrace{0,\cdots,0}_{L_a-1}\end{bmatrix}^{\mathrm{T}}. \quad (96)$$

(96) is formulated to ensure that the rotation matrix $\mathbf{B}$ rotates the vector $\mathbf{N}^{L_a}$ along the same axis as did in (91). With rotation matrix $\mathbf{B}$, we can implement the *coordinates transformations* such that $\left[\mathbf{N}^{L_a}\right]^{\mathrm{T}} = \mathbf{B}^{\mathrm{T}}\left[\mathbf{n}^{L_a}\right]^{\mathrm{T}}$, where $\mathbf{n}^{L_a}$ is the transformed vector consisting of $\{n'_{i,j}\}_{i\in[n/k],j\in[L]}$. Substituting $\left[\mathbf{N}^{L_a}\right]^{\mathrm{T}} = \mathbf{B}^{\mathrm{T}}\left[\mathbf{n}^{L_a}\right]^{\mathrm{T}}$ into (94) yields that

$$\overbrace{\int\cdots\int}^{L_a}_{\mathbf{A}_1[\mathbf{N}^{L_a}]^{\mathrm{T}} \le -\frac{\|\mathbf{g}\|}{2}} \frac{1}{\left(\sqrt{2\pi\sigma^2}\right)^{L_a}}e^{-\frac{\|\mathbf{N}^{L_a}\|^2}{2\sigma^2}}\prod_{i=a}^{n/k}\prod_{j=1}^{L}dn_{i,j} =$$
$$\overbrace{\int\cdots\int}^{L_a}_{\mathbf{A}_1\mathbf{B}^{\mathrm{T}}[\mathbf{n}^{L_a}]^{\mathrm{T}} \le -\frac{\|\mathbf{g}\|}{2}} \frac{e^{-\frac{\mathbf{n}^{L_a}\mathbf{B}\mathbf{B}^{\mathrm{T}}[\mathbf{n}^{L_a}]^{\mathrm{T}}}{2\sigma^2}}}{\left(\sqrt{2\pi\sigma^2}\right)^{L_a}} \cdot \left|\mathbf{J}\left(\mathbf{n}^{L_a}\right)\right|\prod_{i=a}^{n/k}\prod_{j=1}^{L}dn'_{i,j}, \quad (97)$$

where $\mathbf{J}\left(\mathbf{n}^{L_a}\right)$ is the *Jacobi matrix*, given as

$$\mathbf{J}\left(\mathbf{n}^{L_a}\right) = \begin{bmatrix}\frac{\partial n'_{a,1}}{\partial n_{a,1}} & \cdots & \frac{\partial n'_{a,1}}{\partial n_{n/k,L}} \\ \vdots & \ddots & \vdots \\ \frac{\partial n'_{n/k,L}}{\partial n_{a,1}} & \cdots & \frac{\partial n'_{n/k,L}}{\partial n_{n/k,L}}\end{bmatrix}. \quad (98)$$

As $\left[\mathbf{N}^{L_a}\right]^{\mathrm{T}} = \mathbf{B}^{\mathrm{T}}\left[\mathbf{n}^{L_a}\right]^{\mathrm{T}}$, we have that $\left[\mathbf{n}^{L_a}\right]^{\mathrm{T}} = \mathbf{B}\left[\mathbf{N}^{L_a}\right]^{\mathrm{T}}$, and thus the Jacobi matrix is simply

$$\mathbf{J}\left(\mathbf{n}^{L_a}\right) = \mathbf{B}. \quad (99)$$

Recall that $\mathbf{B}$ is a rotation matrix, we obtain that $\left|\mathbf{J}\left(\mathbf{n}^{L_a}\right)\right|^2 = |\mathbf{B}|^2 = \left|\mathbf{B}\mathbf{B}^{\mathrm{T}}\right| = \left|\mathbf{I}_{L_a}\right| = 1$ and thus $\left|\mathbf{J}\left(\mathbf{n}^{L_a}\right)\right| = 1$. Also, we could let $\mathbf{A}_1 = \mathbf{B}_1$ without loss of generality. This

characteristic yields the following equation.

$$
\begin{aligned}
\mathbf{A}_1 \mathbf{B}^{\mathrm{T}} &= \left[\begin{array}{cccc} \mathbf{A}_1 \mathbf{B}_1^{\mathrm{T}} & \mathbf{A}_1 \mathbf{B}_2^{\mathrm{T}} & \cdots & \mathbf{A}_1 \mathbf{B}_{L_a}^{\mathrm{T}} \end{array}\right] \\
&= \left[\begin{array}{cccc} \mathbf{B}_1 \mathbf{B}_1^{\mathrm{T}} & \mathbf{B}_1 \mathbf{B}_2^{\mathrm{T}} & \cdots & \mathbf{B}_1 \mathbf{B}_{L_a}^{\mathrm{T}} \end{array}\right] \\
&\stackrel{(a)}{=} \left[1, \underbrace{0, \cdots, 0}_{L_a}\right],
\end{aligned}
\tag{100}
$$

where (a) is obtained from the property of rotation matrix such that $\mathbf{B}\mathbf{B}^{\mathrm{T}} = \mathbf{I}_{L_a}$. Then, applying (100) and (98) in (97) results in the following simplification:

$$
\begin{aligned}
&\overbrace{\int \cdots \int}^{L_a}_{\mathbf{A}_1\mathbf{B}^{\mathrm{T}}[\mathbf{n}^{L_a}]^{\mathrm{T}} \le -\frac{\|\mathbf{g}\|}{2}} \frac{e^{-\frac{\mathbf{n}^{L_a}\mathbf{B}\mathbf{B}^{\mathrm{T}}[\mathbf{n}^{L_a}]^{\mathrm{T}}}{2\sigma^2}}}{\left(\sqrt{2\pi\sigma^2}\right)^{L_a}} \cdot \left|\mathbf{J}\left(\mathbf{n}^{L_a}\right)\right| \prod_{i=a}^{n/k} \prod_{j=1}^{L} dn'_{i,j} \\
&= \overbrace{\int \cdots \int}^{L_a}_{[1,0,\cdots,0][\mathbf{n}^{L_a}]^{\mathrm{T}} \le -\frac{\|\mathbf{g}\|}{2}} \frac{1}{\left(\sqrt{2\pi\sigma^2}\right)^{L_a}} e^{-\frac{\|\mathbf{n}^{L_a}\|^2}{2\sigma^2}} \prod_{i=a}^{n/k} \prod_{j=1}^{L} dn'_{i,j} \\
&= \overbrace{\int \cdots \int}^{L_a}_{n'_{a,1} \le -\frac{\|\mathbf{g}\|}{2}} \frac{1}{\left(\sqrt{2\pi\sigma^2}\right)^{L_a}} e^{-\frac{\|\mathbf{n}^{L_a}\|^2}{2\sigma^2}} \prod_{i=a}^{n/k} \prod_{j=1}^{L} dn'_{i,j} \\
&= \int_{-\infty}^{-\frac{\|\mathbf{g}\|}{2}} \frac{1}{\sqrt{2\pi\sigma^2}} e^{-\frac{(n'_{a,1})^2}{2\sigma^2}} dn'_{a,1} = Q\left(\frac{\|\mathbf{g}\|}{2\sigma}\right).
\end{aligned}
\tag{101}
$$

APPENDIX F
PROOF OF LEMMA 9

Substitute (72) into (16), proving the asymptotic inequality given in (70) is equivalent to proving

$$
\lim_{\gamma \to \infty} \mathscr{F}(L_a, \gamma) - \left[2^{-2c} \sum_{i \in \Omega} \sum_{j \in \Omega} \exp\left(-\frac{(i-j)^2}{8\sigma^2}\right)\right]^{L_a} < 0.
\tag{102}
$$

where $\mathscr{F}(L_a, \gamma)$ is given in (16), with the second term's limit given as

$$
\lim_{\gamma \to \infty} \frac{L_a \mathscr{G}(L_a, \gamma)}{\Gamma\left(1 + \frac{L_a}{2}\right)\left(\sqrt{2}\right)^{L_a}} = 0.
\tag{103}
$$

and the first term upper bounded by

$$
\frac{\pi^{L_a/2} L_a \mathscr{H}(L_a, \gamma)}{\Gamma^2\left(1 + \frac{L_a}{2}\right)\left(\sqrt{24\gamma}\right)^{L_a}} < \frac{\pi^{L_a/2} L_a \mathcal{I}_{L_a-1}}{\Gamma^2\left(1 + \frac{L_a}{2}\right)\left(\sqrt{24\gamma}\right)^{L_a}}
\tag{104}
$$

Thus, the LHS of (102) is upper bounded by

$$
\lim_{\gamma \to \infty} \frac{\pi^{L_a/2} L_a \mathcal{I}_{L_a-1}}{\Gamma^2\left(1 + \frac{L_a}{2}\right)\left(\sqrt{24\gamma}\right)^{L_a}} - 2^{-cL_a} = -2^{-cL_a} < 0.
\tag{105}
$$

We thus establish the inequality in (102).

APPENDIX G
PROOF OF LEMMA 12

Let $r = \sigma x$, we can obtain that

$$
\int_0^{\mathcal{D}} r^{2L_a - 1} e^{-\frac{r^2}{2\sigma^2}} dr \stackrel{r=\sigma x}{=} \sigma^{2L_a} \cdot \int_0^{\mathcal{D}/\sigma} x^{2L_a - 1} e^{-\frac{x^2}{2}} dx.
\tag{106}
$$

Thus, the task at hand is to solve the integral $\int_0^{\mathcal{D}/\sigma} x^{2L_a-1} e^{-\frac{x^2}{2}} dx$. We commence our analysis by examining the indefinite integral $\int x^{2L_a-1} e^{-\frac{x^2}{2}} dr$. To solve this integral, we systematically apply the method of *integration by parts*, progressing iteratively from $n = 1$ to $n = L_a$:

$$
\int x^{2n-1} e^{-\frac{x^2}{2}} dx = -x^{2L_a-2} e^{-\frac{x^2}{2}} + (2L_a - 2) \int x^{2L_a-3} e^{-\frac{x^2}{2}} dx,
\tag{107}
$$

Hence, let $a_n(x) = \int x^n e^{-\frac{x^2}{2}} dx$ and we obtain the recurrence relation that

$$
\begin{aligned}
a_{2n-1}(x) &= -x^{2n-2} e^{-\frac{x^2}{2}} + (2n-2) a_{2n-3}(x), n \in \mathbb{N}^+ \\
a_1(x) &= -e^{-\frac{x^2}{2}} + C.
\end{aligned}
\tag{108}
$$

By solving the recursive relation in (108), we could obtain the explicit expression of $a_{2n-1}(x)$ as:

$$
a_{2n-1}(x) = -e^{\frac{-x^2}{2}} \sum_{i=1}^{n} x^{2(n-i)} \prod_{j=1}^{i-1} 2(n-j) + C_1.
\tag{109}
$$

As such, the indefinite integral $\int x^{2L_a-1} e^{-\frac{x^2}{2}} dr$ equals to $a_{2n-1}(x)$. Applying (109) in (106) results in the solution that

$$
\begin{aligned}
&\int_0^{\mathcal{D}} r^{2L_a-1} e^{-\frac{r^2}{2\sigma^2}} dr = \sigma^{2L_a} \left(a_{2L_a-1}(\mathcal{D}/\sigma) - a_{2L_a-1}(0)\right) \\
&= \sigma^{2L_a} \left(-e^{\frac{-\mathcal{D}^2}{2\sigma^2}} \sum_{i=1}^{L_a} \frac{\mathcal{D}^{2(L_a-i)}}{\sigma^{2(L_a-i)}} \prod_{j=1}^{i-1} 2(n-j) + \prod_{j=1}^{L_a-1} 2(n-j)\right).
\end{aligned}
\tag{110}
$$

Let $\mathcal{I}_i \triangleq \prod_{j=1}^{i} 2(L_a - j)$ and we can simplify the RHS of (110) as

$$
\sigma^{2L_a} \left(-e^{\frac{-\mathcal{D}^2}{2\sigma^2}} \sum_{i=1}^{L_a} \frac{\mathcal{D}^{2(L_a-i)}}{\sigma^{2(L_a-i)}} \mathcal{I}_{i-1} + \mathcal{I}_{L_a-1}\right).
\tag{111}
$$

APPENDIX H
PROOF OF LEMMA 13

Let $r = \sigma x$, we obtain that

$$
\int_{\mathcal{D}}^{\infty} r^{L_a-1} e^{-\frac{r^2}{2\sigma^2}} dr \stackrel{r=\sigma x}{=} \sigma^{L_a} \cdot \int_{\mathcal{D}/\sigma}^{\infty} x^{L_a-1} e^{-\frac{x^2}{2}} dx.
\tag{112}
$$

The solution to the indefinite integral $\int x^{L_a-1} e^{-\frac{x^2}{2}} dx$ hinges on the value of L_a, which leads to two distinct scenarios. In the case where L_a is even, the solution can be derived from

This article has been accepted for publication in IEEE Transactions on Communications. This is the author's version which has not been fully edited and content may change prior to final publication. Citation information: DOI 10.1109/TCOMM.2024.3435391

15

(109):

$$\int x^{L_a-1} e^{-\frac{x^2}{2}} dx = a_{L_a-1}(x) \overset{L_a=2n}{=} a_{2n-1}(x)$$

$$= -\sum_{i=1}^{n} x^{2(n-i)} \prod_{j=1}^{i-1} 2(n-j) e^{\frac{-x^2}{2}} + C_1 \tag{113}$$

$$\overset{n=\frac{L_a}{2}}{=} -\sum_{i=1}^{L_a/2} x^{2(L_a/2-i)} \prod_{j=1}^{i-1} 2(L_a/2-j) e^{\frac{-x^2}{2}} + C_1.$$

Let $\mathcal{K}_i \triangleq \prod_{j=1}^{i} (L_a - 2j)$, and the definite integral $\int_{\mathcal{D}/\sigma}^{\infty} x^{L_a-1} e^{-\frac{x^2}{2}} dx$ can be calculated by

$$\exp\left\{\frac{-\mathcal{D}^2}{2\sigma^2}\right\} \sum_{i=1}^{L_a/2} \frac{\mathcal{D}^{(L_a-2i)}}{\sigma^{(L_a-2i)}} \mathcal{K}_{i-1}. \tag{114}$$

In the case where L_a is odd, notice that $a_{L_a-1}(x) \overset{L_a=2n+1}{=} a_{2n}(x)$, we can iteratively introduce the *integration by parts* and obtain the recurrence relations:

$$a_{2n}(x) = -x^{2n-1} e^{-\frac{x^2}{2}} + (2n-1) a_{2n-3}(x), n \in \mathbb{N}^+,$$
$$a_0(x) = \int e^{-\frac{x^2}{2}} dx. \tag{115}$$

By solving the above recursive formula, we obtain the explicit expression of $a_{2n}(x)$:

$$-\sum_{i=1}^{n} x^{2(n-i)+1} \prod_{j=1}^{i-1} (2(n-j)+1) e^{\frac{-x^2}{2}} + \prod_{j=1}^{n-1} (2(n-j)+1) a_0(x). \tag{116}$$

As such, the indefinite could be expressed by

$$\int x^{L_a-1} e^{-\frac{x^2}{2}} dx = a_{L_a-1}(x) \overset{L_a=2n+1}{=} a_{2n}(x)$$

$$= -e^{\frac{-x^2}{2}} \sum_{i=1}^{(L_a-1)/2} x^{L_a-2i} \mathcal{K}_{i-1} + a_0(x) \mathcal{K}_{(L_a-3)/2}. \tag{117}$$

Note that

$$\lim_{x \to \infty} a_0(x) - a_0(\mathcal{D}/\sigma) = \sqrt{2\pi} Q(\mathcal{D}/\sigma), \tag{118}$$

The definite integral in the RHS of (112) is then given as:

$$\int_{\mathcal{D}/\sigma}^{\infty} x^{L_a-1} e^{-\frac{x^2}{2}} dx$$

$$= e^{\frac{-\mathcal{D}^2}{2\sigma^2}} \sum_{i=1}^{(L_a-1)/2} \frac{\mathcal{D}^{L_a-2i}}{\sigma^{L_a-2i}} \mathcal{K}_{i-1} + \mathcal{K}_{(L_a-3)/2} \int_{\mathcal{D}/\sigma}^{\infty} e^{-\frac{x^2}{2}} dx$$

$$= e^{\frac{-\mathcal{D}^2}{2\sigma^2}} \sum_{i=1}^{(L_a-1)/2} \frac{\mathcal{D}^{L_a-2i}}{\sigma^{L_a-2i}} \mathcal{K}_{i-1} + \sqrt{2\pi} Q(\mathcal{D}/\sigma) \mathcal{K}_{(L_a-3)/2}. \tag{119}$$

Substitute (119) into (112) and we obtain the solution.

REFERENCES

[1] R. G. Gallager, *Information theory and reliable communication*. Wiley, 1968.

[2] X. Yu, Y. Li, W. Yang, and Y. Sun, "Design and analysis of unequal error protection rateless Spinal Codes," *IEEE Trans. Commun.*, vol. 64, no. 11, pp. 4461–4473, 2016.

[3] H. Balakrishnan, P. Iannucci, J. Perry, and D. Shah, "De-randomizing shannon: The design and analysis of a capacity-achieving rateless code," *arXiv preprint arXiv:1206.0418*, 2012.

[4] J. Perry, H. Balakrishnan, and D. Shah, "Rateless Spinal codes," *Proc. ACM HotNets*, pp. 1–6, 2011.

[5] J. Perry, P. A. Iannucci, K. E. Fleming, H. Balakrishnan, and D. Shah, "Spinal codes," *Proc. ACM SIGCOMM 2012*, pp. 49—-60, 2012.

[6] R. Gallager, "Low-density parity-check codes," *IRE Trans. Inf. Theory*, vol. 8, no. 1, pp. 21–28, 1962.

[7] A. Shokrollahi, "Raptor codes," *IEEE Trans. Inf. Theory*, vol. 52, no. 6, pp. 2551–2567, 2006.

[8] A. Gudipati and S. Katti, "Strider: Automatic rate adaptation and collision handling," *Proc. ACM SIGCOMM 2011*, pp. 158—-169, 2011.

[9] M. Vaezi, A. Azari, S. R. Khosravirad, M. Shirvanimoghaddam, M. M. Azari, D. Chasaki, and P. Popovski, "Cellular, wide-area, and non-terrestrial IoT: A survey on 5G advances and the road toward 6G," *IEEE Commun. Surv. Tutorials*, vol. 24, no. 2, pp. 1117–1174, 2022.

[10] S. Wu, D. Li, J. Jiao, and Q. Zhang, "CS-LTP-Spinal: A cross-layer optimized rate-adaptive image transmission system for deep-space exploration," *Sci. China Inf. Sci.*, vol. 65, no. 1, 2022.

[11] H. Liang, A. Liu, X. Tong, and C. Gong, "Raptor-like rateless spinal codes using outer systematic polar codes for reliable deep space communications," in *IEEE INFOCOM Workshops*, 2020, pp. 1045–1050.

[12] N. Deng, X. Shi, M. Sheng, J. Liu, H. Wei, N. Zhao, and D. Niyato, "Enhancing millimeter wave cellular networks via uav-borne aerial IRS swarms," *IEEE Trans. Commun.*, vol. 72, no. 1, pp. 524–538, 2024.

[13] L. Wang, Y. L. Che, L. Duan, and K. Wu, "Multiple access mmwave design for uav-aided 5g communications," *IEEE Wirel. Commun.*, vol. 26, no. 1, pp. 64–71, 2019.

[14] X. Pang, M. Liu, Z. Li, Z. Jiao, and S. Sun, "Trust function based spinal codes over the mobile fading channel between UAVs," in *Proc. IEEE GLOBECOM*, 2018, pp. 1–7.

[15] X. Shi and N. Deng, "Modeling and analysis of mmwave UAV swarm networks: A stochastic geometry approach," *IEEE Trans. Wirel. Commun.*, vol. 21, no. 11, pp. 9447–9459, 2022.

[16] P. A. Iannucci, J. Perry, H. Balakrishnan, and D. Shah, "No symbol left behind: a link-layer protocol for rateless codes," in *Proc. ACM Mobicom*, 2012, pp. 17–28.

[17] J. Xu, S. Wu, J. Jiao, and Q. Zhang, "Optimized Puncturing for the Spinal Codes," in *Proc. IEEE ICC*, 2019, pp. 1–5.

[18] A. Li, S. Wu, Y. Wang, J. Jiao, and Q. Zhang, "Spinal codes over BSC: Error probability analysis and the puncturing design," in *Proc. IEEE VTC2020-Spring*, 2020, pp. 1–5.

[19] X. Yu, Y. Li, and W. Yang, "Superposition Spinal codes with unequal error protection property," *IEEE Access*, vol. 5, pp. 6589–6599, 2017.

[20] W. Yang, Y. Li, X. Yu, and Y. Sun, "Two-way Spinal codes," in *Proc. IEEE ISIT*, 2016, pp. 1919–1923.

[21] X. Yu, Y. Li, and W. Yang, "Superposition spinal codes with unequal error protection property," *IEEE Access*, vol. 5, pp. 6589–6599, 2017.

[22] A. Li, S. Wu, J. Jiao, N. Zhang, and Q. Zhang, "Spinal codes over fading channel: Error probability analysis and encoding structure improvement," *IEEE Trans. Wirel. Commun.*, vol. 20, no. 12, pp. 8288–8300, 2021.

[23] S. Meng, S. Wu, A. Li, J. Jiao, N. Zhang, and Q. Zhang, "Partial self-concatenation structure and performance analysis of Spinal codes over rayleigh fading channel," *IEEE Trans. Veh. Technol.*, vol. 71, no. 6, pp. 6767–6771, 2022.

[24] X. Xu, S. Wu, D. Dong, J. Jiao, and Q. Zhang, "High performance short polar codes: A concatenation scheme using spinal codes as the outer code," *IEEE Access*, vol. 6, pp. 70 644–70 654, 2018.

[25] H. Liang, A. Liu, X. Tong, and C. Gong, "Raptor-like rateless spinal codes using outer systematic polar codes for reliable deep space communications," in *IEEE INFOCOM Workshops*, 2020, pp. 1045–1050.

[26] D. Dong, S. Wu, X. Jiang, J. Jiao, and Q. Zhang, "Towards high performance short polar codes: Concatenated with the Spinal codes," in *Proc. IEEE PIMRC*, 2017, pp. 1–5.

[27] Y. Cao, F. Du, J. Zhang, and X. Peng, "Polar-UEP Spinal concatenated encoding in free-space optical communication," *Applied Optics*, vol. 61, no. 1, pp. 273–278, 2022.

[28] Y. Li, J. Wu, B. Tan, M. Wang, and W. Zhang, "Compressive Spinal codes," *IEEE Trans. Veh. Technol.*, vol. 68, no. 12, pp. 11 944–11 954, 2019.

This article has been accepted for publication in IEEE Transactions on Communications. This is the author's version which has not been fully edited and content may change prior to final publication. Citation information: DOI 10.1109/TCOMM.2024.3435391

16

[29] Y. Hu, R. Liu, H. Bian, and D. Lyu, "Design and analysis of a low-complexity decoding algorithm for Spinal codes," *IEEE Trans. Veh. Technol.*, vol. 68, no. 5, pp. 4667–4679, 2019.

[30] S. Xu, S. Wu, J. Luo, J. Jiao, and Q. Zhang, "Low complexity decoding for spinal codes: Sliding feedback decoding," in *Proc. IEEE VTC-Fall*. IEEE, 2017, pp. 1–5.

[31] W. Yang, Y. Li, X. Yu, and J. Li, "A low complexity sequential decoding algorithm for rateless spinal codes," *IEEE Commun. Lett.*, vol. 19, no. 7, pp. 1105–1108, 2015.

[32] S. Meng, S. Wu, A. Li, J. Jiao, N. Zhang, and Q. Zhang, "Analysis and optimization of the harq-based spinal coded timely status update system," *IEEE Transactions on Communications*, vol. 70, no. 10, pp. 6425–6440, 2022.

[33] ——, "Analysis and optimization of spinal codes over the bsc: from the aoi perspective," in *2021 IEEE International Conference on Communications Workshops (ICC Workshops)*, 2021, pp. 1–6.

[34] F. Lázaro, G. Liva, G. Bauch, and E. Paolini, "Bounds on the error probability of Raptor codes under maximum likelihood decoding," *IEEE Trans. Inf. Theory*, vol. 67, no. 3, pp. 1537–1558, 2021.

[35] D. Goldin and D. Burshtein, "Performance bounds of concatenated Polar coding schemes," *IEEE Trans. Inf. Theory*, vol. 65, no. 11, pp. 7131–7148, 2019.

[36] B. Shuval and I. Tal, "A lower bound on the probability of error of Polar codes over BMS channels," *IEEE Trans. Inf. Theory*, vol. 65, no. 4, pp. 2021–2045, 2019.

[37] B. Schotsch, G. Garrammone, and P. Vary, "Analysis of LT codes over finite fields under optimal erasure decoding," *IEEE Commun. Lett.*, vol. 17, no. 9, pp. 1826–1829, 2013.

[38] B. Schotsch, *Rateless coding in the finite length regime*. Hochschulbibliothek der Rheinisch-Westfälischen Technischen Hochschule Aachen, 2014.

[39] I. Sason and S. Shamai, "Performance analysis of linear codes under maximum-likelihood decoding: A tutorial," *Found. Trends Commun. Inf. Theory*, vol. 3, no. 1–2, pp. 1–222, 2006.

[40] H. Solomon, *Geometric Probability*. SIAM, 1978, vol. 28.

[41] J. W. Craig, "A new, simple and exact result for calculating the probability of error for two-dimensional signal constellations," in *Proc. IEEE MILCOM*, 1991, pp. 571–575.

Xiaomeng Chen received her B.E. degree in electronic and information engineering from the Harbin Institute of Technology (Shenzhen) in 2023, where she was awarded the highest honor of Undergraduate Thesis. She is currently pursuing her M.S. degree with the Department of Electronic Engineering, HITSZ. Her research interests include advanced channel coding techniques, wireless communications, and information theory.

Sumei Sun (Fellow, IEEE) is Executive Director of the Institute for Infocomm Research (I2R), Agency for Science, Technology, and Research (A*STAR), Singapore. She also holds an adjunct appointment with the National University of Singapore, and joint appointment with the Singapore Institute of Technology, both as a full professor. Her current research interests include next-generation wireless communications, joint communication-sensing-computing-control design, industrial internet of things, applied deep learning and artificial intelligence. She has been Member-at-Large of the IEEE Communications Society and is a member of the IEEE Vehicular Technology Society Board of Governors (2022-2024), Fellow of the IEEE and the Academy of Engineering Singapore.

Aimin Li (Student Member, IEEE) received his B.E. from Harbin Institute of Technology Shenzhen (HITSZ) in 2020, where he was awarded the highest honor of Undergraduate Thesis. He is currently a Ph.D student at HITSZ and a visit student at Institute for Infocomm Research (I2R), Agency for Science, Technology, and Research (A*STAR). He has served as a Reviewer for IEEE TWC, IEEE TNNLS, IEEE TVT, IEEE CL, IEEE ISIT, *etc.* His current research interests include channel coding, age of information and goal-oriented semantic communications.
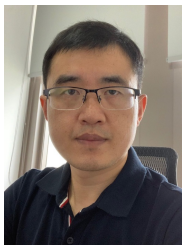
Shaohua Wu (Member, IEEE) received the Ph.D. degree in communication engineering from Harbin Institute of Technology, Harbin, China, in 2009. From 2009 to 2011, he held a postdoctoral position with the Department of Electronics and Information Engineering, Shenzhen Graduate School, Harbin Institute of Technology, where he has been with since 2012. From 2014 to 2015, he was a Visiting Researcher with BBCR, University of Waterloo, Canada. He is currently a Full Professor with the Harbin Institute of Technology (Shenzhen), China. He is also a Professor with Pengcheng Laboratory, Shenzhen, China. His research interests include satellite and space communications, advanced channel coding techniques, space-air-ground-sea integrated networks, and B5G/6G wireless transmission technologies. He has authored or coauthored over 100 papers in these fields and holds over 40 Chinese patents.